Supporting Information

Hit optimization by dynamic combinatorial chemistry on *Streptococcus pneumoniae* energy-coupling factor transporter ECF-PanT

Ioulia Antonia Exapicheidou, ‡[a,b] Atanaz Shams, ‡[a, b] Hamza Ibrahim,[c] Aleksei Tsarenko,[d] Michael Backenköhler,[c] Mostafa Hamed,[a] Eleonora Diamanti,[a] Andrea Volkamer,[a,c] Dirk J. Slotboom,[d] Anna K. H. Hirsch*[a, b]

[a] *Helmholtz Institute for Pharmaceutical Research Saarland (HIPS) – Helmholtz Centre for Infection Research (HZI), 66123, Saarbrücken, Germany.*
[b] *Saarland University, Department of Pharmacy, Campus Building E8.1, 66123, Saarbrücken, Germany.*
[c] *Data Driven Drug Design Group, Center for Bioinformatics, Saarland Informatics Campus E2.1, Saarland University, 66123 Saarbrücken, Germany*
[d] *Groningen Biomolecular Sciences and Biotechnology Institute, University of Groningen, Nijenborgh 4, 9747, AG, Groningen, The Netherlands.*
†Electronic Supplementary Information (ESI) available.
See DOI: 10.1039/x0xx00000x

*Corresponding author
Prof. A. K. H. Hirsch
e-mail: anna.hirsch@helmholtz-hips.de

Table of Contents

General information

All reactions using oxygen- and/or moisture-sensitive materials were carried out in dry solvents (*vide infra*) under a nitrogen atmosphere using oven-dried glassware. Reactions were monitored by a liquid chromatography-mass spectrometry (LC-MS) system equipped with a Dionex UltiMate 3000 pump, autosampler, column compartment, detector, and ESI quadrupole MS (MSQ Plus or ISQ EC) from Thermo Fisher Scientific, Dreieich, Germany. Purification of the final products, when necessary, was performed using preparative HPLC (Dionex UltiMate 3000 UHPLC+ focused, Thermo Scientific) on a reversed-phase column (C18 column, 5 µM, Macherey-Nagel, Germany). The solvents used for the chromatography were water (0.1% formic acid) and MeCN (0.1% formic acid). High-resolution mass (HRMS) of final products was determined by LCMS/MS using a Thermo Scientific Q Exactive Focus Orbitrap LC-MS/MS system. NMR data were collected on a Bruker Avance Neo 500 MHz (^{1}H at 500.0 MHz; ^{13}C at 126.0 MHz; ^{19}F NMR at 470 MHz), equipped with a Prodigy Cryo-probe. Chemical shifts are reported in parts per million (ppm) relative to residual solvent peak (DMSO-d_6, ^{1}H: 2.54 ppm; ^{13}C: 39.9 ppm). Coupling constants are reported in Hertz (Hz). Multiplicity is reported with the usual abbreviations (s: singlet, br s: broad singlet, d: doublet, dd: doublet of doublets, ddd: doublet of doublet of doublets, t: triplet, dt: doublet of triplets, q: quartet, p: pentet, dp: doublet of pentets, m: multiplet). The periodic progress and analysis of DCC experiments were monitored by UPLC-MS (ThermoScientific Dionex Ultimate 3000 UHPLC System coupled to a ThermoScientific Q Exactive Focus with an electrospray ion source) using an Acquity Waters Column (BEH, C8 1.7 µm, 2.1 × 150 mm, Waters, Germany) at a flow rate of 0.250 mL/min with detection set at 210, 254, 290, and 310 nm, and the mass spectrum recorded in a positive mode in the range of 100−700 m/z. The solvent system was 0.1% formic acid in H_2O (Solvent-A) and 0.1% formic acid in MeCN (Solvent-B). The gradient program began with 5% of Solvent-B for 1 min and was then increased to 95% of Solvent-B over 17 min and held for 2 min, followed by a decrease of Solvent-B to 5% over 0.1 min, where it was held for 2 min. Compounds were purified by prep. HPLC eluting with an alternating gradient of 5–100% ACN with 0.05% FA in H_2O with 0.05% FA. All the compounds have a purity > 95% according to LC-MS.

Chemicals

Unless indicated otherwise, reagents and substrates were purchased from commercial sources and used as received. Solvents not required to be dry were purchased as technical-grade and used as received. All new compounds were fully characterized by ^{1}H- and ^{13}C-NMR and HRMS techniques. The purity of all the final products was determined by LC-MS and found to be >95%.

General procedure for DCC experiments

DCL preparation (GP-1):

To a 1.5 mL Eppendorf Tube® containing phosphate buffer (Phosphate buffer, pH 7.5) were added hydrazides (150 μM each, in DMSO), aldehydes (50 μM each, in DMSO), aniline (5 mM, in DMSO), and an additional amount of DMSO to reach a final concentration of 5% in the DCL with 500 μL of end-volume. The DCL was allowed to gently mix on a rotating wheel (7 rpm) at room temperature and was frequently monitored via UPLC-MS. For analysis, 20 μL of the corresponding library was mixed with 28 μL acetonitrile and 2 μL of NaOH (2 M), the mixture was centrifuged, and the supernatant was used for the analysis.[1]

Protein-templated DCL preparation (GP-2):

To a 1.5 mL Eppendorf Tube® containing phosphate buffer (pH 7.5) were added hydrazides (150 μM each, in DMSO), aldehydes (50 μM each, in DMSO), aniline (5mM, in DMSO), *Streptococcus pneumoniae* ECF-PanT (11.77 – 13.17 μM) in phosphate buffer at pH 7.5,[2] and an additional amount of DMSO to reach a final concentration of 5% in the DCL with 500 μL of end-volume. The DCL with the protein was allowed to gently mix on a rotating wheel (7 rpm) at room temperature, was frequently monitored via UPLC-MS ,and the traces were compared with the blank composition. For analysis, 20 μL of the corresponding library were mixed with 28 μL acetonitrile and 2 μL of NaOH (2 M), the mixture was centrifuged and the supernatant was used for the analysis.[1]
Note: The protein-templated DCL-1, -2 and -3 were run as duplicates.

Assessment of DCL composition

The library composition was assessed after the equilibrium of acylhydrazone formation was reached as reported in the literature. All the DCLs in this study reached an equilibrium after four to twenty eight hours. The "amplification factor" was determined with the relative peak area (RPA), which is the percent of each peak when the sum of all peak areas was set to 100%. The "normalized RPA" was used for the final assessment of amplification of the acylhydrazone products in the DCL.[1, 3]

$$amplification\ factor = RPA(templated)\ RPA(blank)$$

$$normalized\ change\ of\ RPA = (RPA(templated) - RPA(blank))\ RPA(blank)$$

DCC-experiments

tdDCC-1 for establishing the DCC conditions using ECF-PanT for the first time:

Initially, we built our first DCL library by choosing a diverse set of commercially available aldehydes and hydrazides with the aim to find the optimal conditions for our protein and at the same time identify new hits as potential ECF inhibitors.
The composition of DCL-1 is depicted in Fig. S1A, ESI† and includes three aldehydes (**A1**—**A3**) and eight differently substituted hydrazides (**H1**—**H8**). From the results of the tdDCL-1, we observed that the products formed did not show significant changes after 28 hours (Fig. S1B, ESI†). Then, the blank library was compared to the two protein-templated ones. The analysis of this experiment showed that the ECF protein altered the equilibrium and, thus, the composition of the DCL, as acylhydrazones **A1H6**, **A1H7**, **A1H5**, **A2H5** and **A3H8** were amplified (Fig. S1, ESI†) and then synthesized for testing.

DCL-1 (20 mol% protein): The DCC-experiment was carried out according to GP-1 (blank) and GP-2 (protein-templated) in phosphate buffer at pH 7.5 and 5% DMSO.

Table 1: Composition of dynamic combinatorial library 1 (DCL-1) of target-directed dynamic combinatorial chemistry experiment 1 (tdDCC-1)

Entry	Blank		Protein-templated (I)		Protein-templated (II)	
	Amount	Final conc. in DCL	Amount	Final conc. in DCL	Amount	Final conc. in DCL
Buffer phosphate pH 7.5*	475 μL	-	222 μL	-	222 μL	-
Aldehyde 100 mM	3 × 5 (15 μL)	(3 × 50 μM)	3 × 5 (15 uL)	(3 × 50 μM)	3 × 5[a] (15 μL)	(3 × 50 μM)
Hydrazide 100 mM	8 × 5 (40 μL)	(8 × 150 μM)	8 × 5 (40 μL)	(8 × 150 μM)	8 × 5[b] (40 μL)	(8 × 150 μM)
Aniline 1M in DMSO	5 μL	5 mM	5 μL	5 mM	5 uL	5 mM
DMSO	13.25 μL	-	13.25 μL	-	13.25 μL	-
Streptococcus pneumoniae ECF-PanT (11.77 uM)	0	-	253 μL	10 μM	253 μL	10 μM

*The buffer is 50mM KP_i, pH= 7.5 with 50 mM NaCl and 0.05 %(w/v) DDM. [a]To minimize the error, the 15 μL stock solution was prepared by mixing 5 μL of each aldehyde from the initial 100 mM stock, and 0.75μL were taken from this stock. [b]To minimize the error, the 40 μL stock solution was prepared by mixing 5 μL of each hydrazide from the initial 100 mM stock, and 6 μL were taken from this stock.

DCC-2:

This experiment library consisted of two aldehydes (**A4**–**A5**) and eight hydrazides (**H9**–**H15**) as shown in S2A.

DCL-2 (20 mol% protein): The DCC-experiment was carried out according to the GP-1 (blank) and GP-2 (protein-templated) in phosphate buffer at pH 7.5 and 5% DMSO.

Table 2: Composition of dynamic combinatorial library 2 (DCL-2) of target-directed dynamic combinatorial chemistry experiment 2 (tdDCC-2)

Entry	Blank		Protein-templated (I)		Protein-templated (II)	
	Amount	Final conc. in DCL	Amount	Final conc. in DCL	Amount	Final conc. in DCL
Buffer phosphate pH 7.5*	475 μL	-	52 μL	-	52 μL	-
Aldehyde 100 mM	2 × 5 (10 μL)	(2 × 50 μM)	2 × 5 (10 μL)	(2 × 50 μM)	2 × 5[a] (10 μL)	(2 × 50 μM)
Hydrazide 100 mM	7 × 5 (35 μL)	(7× 150 μM)	7 × 5 (35 uL)	(7 × 150 μM)	7 × 5[b] (35 μL)	(7 × 150μM)
Aniline 1M in DMSO	5 μL	5 mM	5 μL	5 mM	5 μL	5 mM
DMSO	13.25 μL	-	13.25 μL	-	13.25	-
Streptococcus pneumoniae ECF-PanT (11.77 uM)	0	-	424 μL	10 μM	424 μL	10 μM

*The buffer is 50mM KP_i, pH= 7.5 with 50mM NaCl and 0.05 %(w/v) DDM. [a]To minimize the error, the 10 μL stock solution was prepared by mixing 5 μL of each aldehyde from the initial 100 mM stock, and 0.5 μL were taken from this stock. [b]To minimize the error, the 35 μL stock solution was prepared by mixing 5 μL of each hydrazide from the initial 100 mM stock, and 5.25 μL were taken from this stock.

DCC-3:

This experiment library consists of three aldehydes (**A6**–**A8**) and seven hydrazides (**H1**–**H7**) as shown in S3A.
DCL-3 (20 mol% protein): The DCC-experiment was carried out according to the GP-1 (blank) and GP-2 (protein-templated) in phosphate buffer at pH 7.5 and 5% DMSO. The DCL composition is depicted in Table 3.

Table 3: Composition of dynamic combinatorial library 3 (DCL-3) of target-directed dynamic combinatorial chemistry experiment 3 (tdDCC-3)

Entry	Blank		Protein-templated (I)		Protein-templated (II)	
	Amount	Final conc. in DCL	Amount	Final conc. in DCL	Amount	Final conc. in DCL
Buffer phosphate pH 7.5*	475 μL	-	95.4 μL	-	95.4 μL	-
Aldehyde 100 mM	3 × 5 (15 μL)	(3 × 50 μM)	3 × 5 (15 μL)	(3 × 50 μM)	3 × 5[a] (15 μL)	(3 × 50 μM)
Hydrazide 100 mM	8 × 5 40 μL	(8 × 150 μM)	8 × 5 (40 μL)	(8 × 150 μM)	8 × 5[b] (40 μL)	(8 × 150 μM)
Aniline 1M in DMSO	5 μL	5 mM	5 μL	5 mM	5 μL	5 mM
DMSO	13.25 μL	-	13.25	-	13.25	-
S. pneumoniae ECF-PanT (13.17 uM)	0	-	379.6 μL	10 μM	379.6 μL	10 μM

*The buffer is 50mM KP_i, pH= 7.5 with 50 mM NaCl and 0.05 %(w/v) DDM. [a]To minimize the error, the 15 μL stock solution was prepared by mixing 5 μL of each aldehyde from the initial 100 mM stock, and 0.75μL were taken from this stock. [b] To minimize the error, the 40 μL stock solution was prepared by mixing 5 μL of each hydrazide from the initial 100 mM stock, and 6 μL were taken from this stock.

Target-directed dynamic combinatorial chemistry experiment 1 (tdDCC-1):

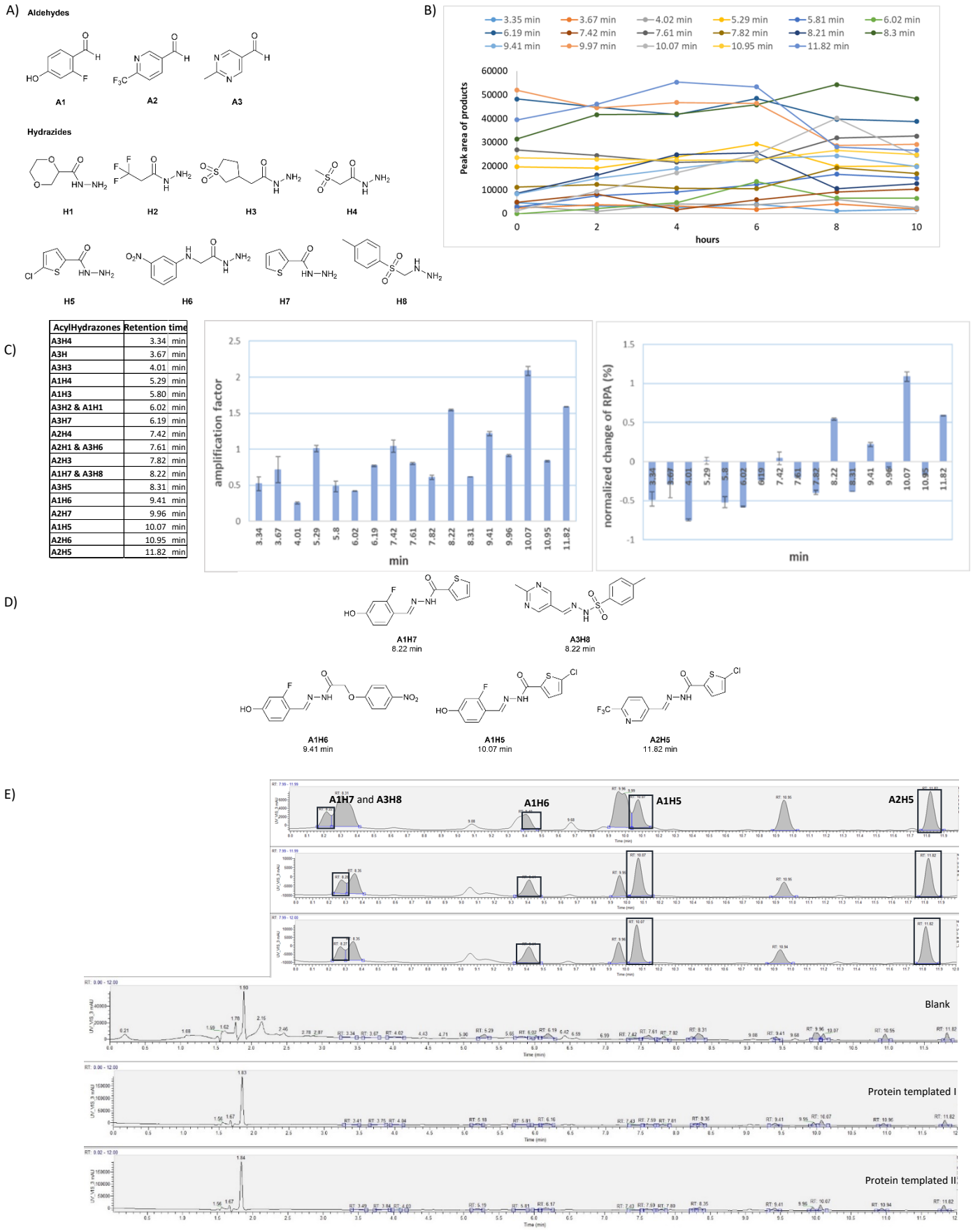

AcylHydrazones	Retention time
A3H4	3.34 min
A3H	3.67 min
A3H3	4.01 min
A1H4	5.29 min
A1H3	5.80 min
A3H2 & A1H1	6.02 min
A3H7	6.19 min
A2H4	7.42 min
A2H1 & A3H6	7.61 min
A2H3	7.82 min
A1H7 & A3H8	8.22 min
A3H5	8.31 min
A1H6	9.41 min
A2H7	9.96 min
A1H5	10.07 min
A2H6	10.95 min
A2H5	11.82 min

Figure S.1. A) Dynamic combinatorial library 1 (DCL-1) composition, B) evaluation of the equilibrium state in the blank DCL-1 by comparing relative peak areas (RPA) of products formed over time, C) amplification factor and normalized change of RPA of products, D) amplified acylhydrazones in protein-templated target-directed dynamic combinatorial chemistry 1 (tdDCC-1). E) Comparison between blank and protein-templated tdDCC-1 samples at twenty-height hours.

Target-directed dynamic combinatorial chemistry experiment 2 (tdDCC-2):

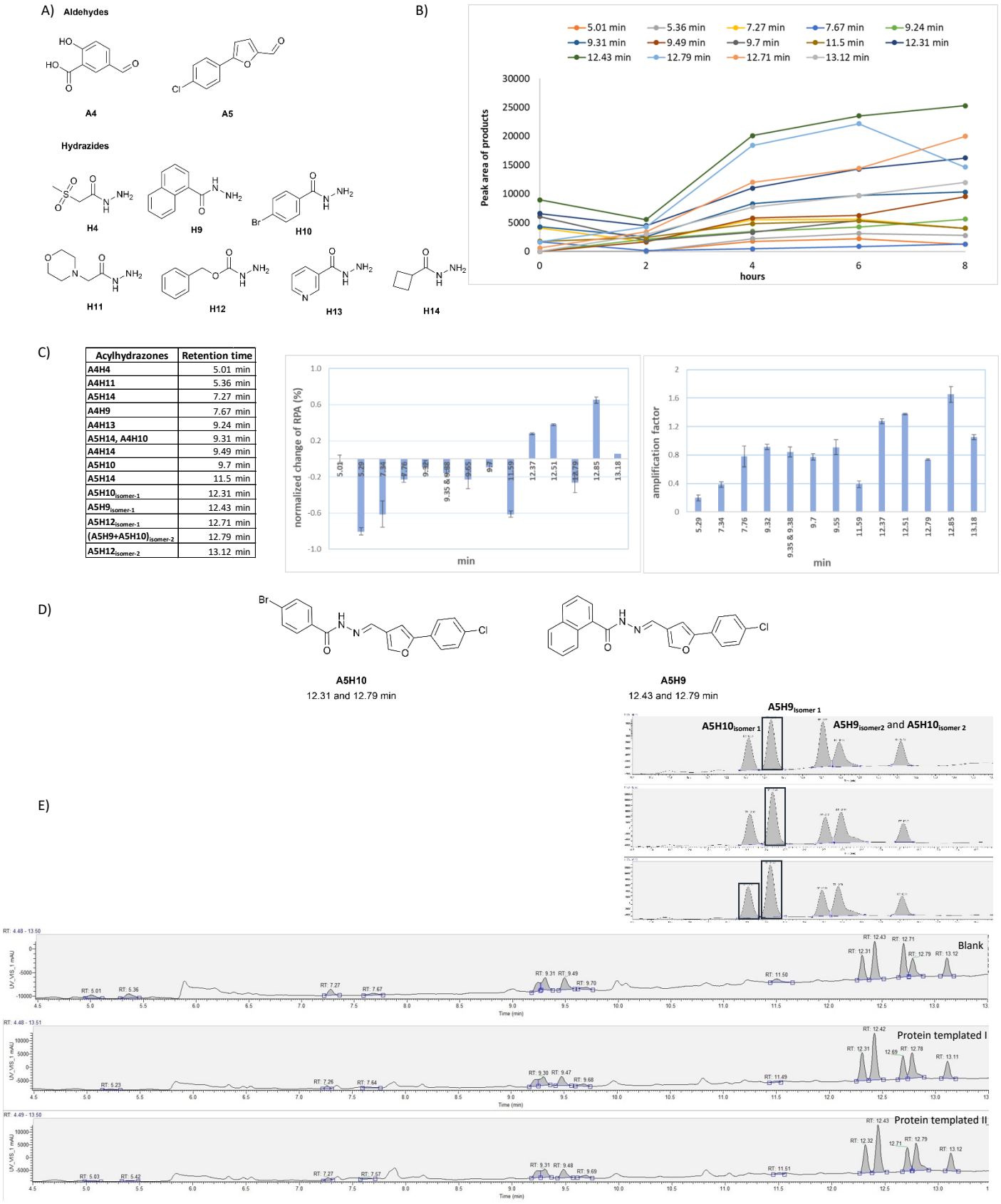

Acylhydrazones	Retention time
A4H4	5.01 min
A4H11	5.36 min
A5H14	7.27 min
A4H9	7.67 min
A4H13	9.24 min
A5H14, A4H10	9.31 min
A4H14	9.49 min
A5H10	9.7 min
A5H14	11.5 min
$A5H10_{isomer-1}$	12.31 min
$A5H9_{isomer-1}$	12.43 min
$A5H12_{isomer-1}$	12.71 min
$(A5H9+A5H10)_{isomer-2}$	12.79 min
$A5H12_{isomer-2}$	13.12 min

Figure S.2. A) Dynamic combinatorial library 2 (DCL-2) composition, B) evaluation of the equilibrium state in the blank DCL-2 by comparing relative peak areas (RPA) of products formed over time, C) amplification factor and normalized change of RPA of products, D) amplified acylhydrazones in protein-templated target-directed dynamic combinatorial chemistry 2 (tdDCC-2). E) Comparison between blank and protein-templated tdDCC-2 samples at twenty-height hours.

Target-directed dynamic combinatorial chemistry experiment 3 (tdDCC-3):

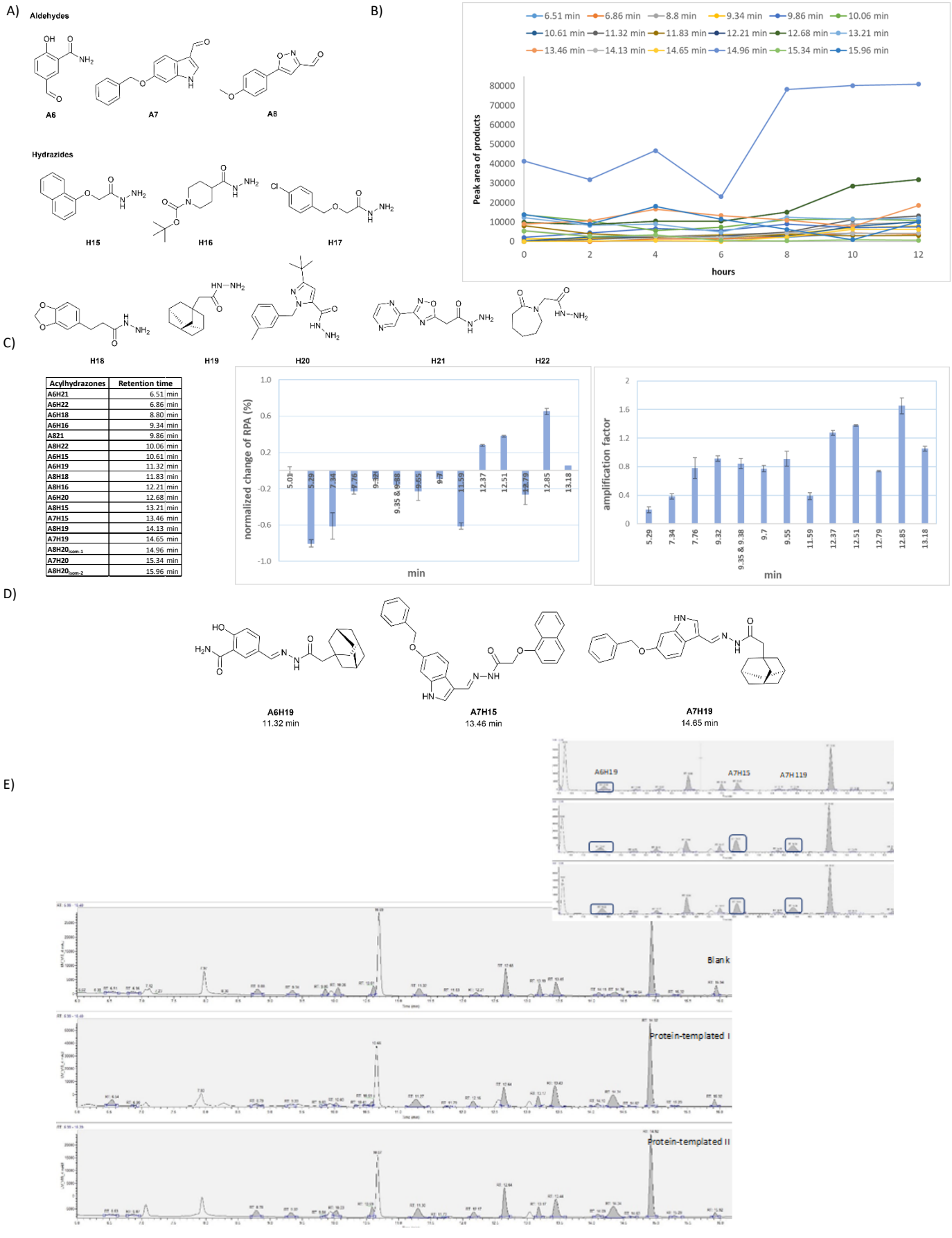

Acylhydrazones	Retention time
A6H21	6.51 min
A6H22	6.86 min
A6H18	8.80 min
A6H16	9.34 min
A821	9.86 min
A8H22	10.06 min
A6H15	10.61 min
A6H19	11.32 min
A8H18	11.83 min
A8H16	12.21 min
A6H20	12.68 min
A8H15	13.21 min
A7H15	13.46 min
A8H19	14.13 min
A7H19	14.65 min
$A8H20_{isom-1}$	14.96 min
A7H20	15.34 min
$A8H20_{isom-2}$	15.96 min

Figure S.3. A) Dynamic combinatorial library 3 (DCL-3) composition, B) evaluation of the equilibrium state in the blank DCL-3 by comparing relative peak areas (RPA) of products formed over time, C) amplification factor and normalized change of RPA of products, D) amplified

acylhydrazones in protein-templated target-directed dynamic combinatorial chemistry 3 (tdDCC-3). E) Comparison between blank and protein-templated tdDCC-3 samples at twenty-height hours.

General procedure for acylhydrazone formation (GP-3):

To a crimp tube equipped with a magnetic stirring bar, the hydrazide (1−1.2 equiv.) and the corresponding aldehyde (1 equiv.) were dissolved/suspended in MeOH (0. 6 M) under a nitrogen atmosphere. The reaction mixture was stirred at 65 °C until complete consumption of the starting material. After cooling the reaction to room temperature, the reaction mixture was precipitated by cooling the crimp tube to 0 °C in an ice bath. The resulting crude was purified by preparative HPLC on a reversed-phase column (C18 column, µM, Macherey-Nagel, Germany) using 15–100% gradient of MeCN (0.05% formic acid) in water (0.05%

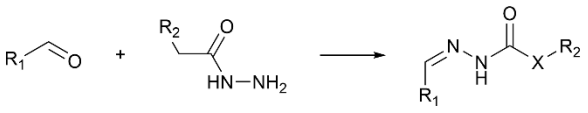

R_1= aromatic group

R_2= aromatic or aliphatic group

X= CH_2, OCH_2, CH_2O, CH_2OCH_2, $(CH_2)_2$, CH_2CH_2, R_2

Scheme 1. General conditions for the synthesis of acylhydrazones.

formic acid), affording the corresponding acylhydrazone products in 60−90% isolated yields.[1]

Characterization of acylhydrazones

Based on ^{1}H-NMR data, the acylhydrazones reported in this work exist as a mixture of cis/trans rotamers in DMSO-d_6 solutions. Thus, ^{1}H-NMR spectra for all compounds show resonances for the CO–NH group protons where the rotamers proton (*cis/trans*) are reported as Ha and Ha'. After reviewing the available literature, it becomes apparent that the acylhydrazones synthesized from aromatic carbaldehydes are essentially planar and exist completely in the form of geometric (*E*)-configuration about the C=N bond due to steric hindrance on the imine bond. Therefore, we discarded the formation of *Z, cis* and *Z, trans* isomers.[4, 5]

(*E*)-1-(5-Chlorothiophen-2-yl)-2-((2-fluoro-4-hydroxybenzylidene)amino)ethan-1-one (A1H5)

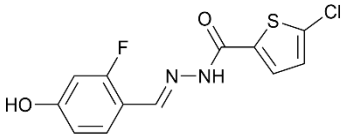

According to GP-3, 2-fluoro-4-hydroxybenzaldehyde **A1** (60 mg, 0.43 mmol) and 2-(4-nitrophenoxy)acetohydrazide **H5** (75.6 mg, 0.42 mmol) were mixed in MeOH (0.7 mL). The crude was purified by preparative HPLC (64% CH_3CN) to afford **A1H5** as a mixture of two rotamers of the amide CO–NH (76:24) as an off-white solid (92.1 mg, 0.428 mmol, 72%). ^{1}H NMR (500 MHz, DMSO-d_6) δ 11.88 (br. s, 2H, 1Ha and 1Ha´), 10.54 (s, 2H, 1Ha and 1Ha´), 8.53 (s, 1H, Ha'), 8.21 (s, 1Ha), 7.88 (d, J = 4.1 Hz, 1H, Ha), 7.83 – 7.69 (m, 3H, 1Ha and 2Ha'), 7.26 (d, J = 4.1 Hz, 2H, 1Ha and 1Ha'), 6.80 (d, J = 8.7 Hz, 1H, Ha), 6.72 (d, J = 8.1 Hz, 1H, Ha'), 6.65 (dt, J = 9.9, 4.9 Hz, 2H, 1Ha and 1Ha'). ^{13}C NMR (126 MHz, DMSO-d_6) δ 162.9, 161.3, 161.2, 160.9, 159.8, 156.5, 141.2, 138.3, 138.3, 137.6, 137.2, 134.3, 133.8, 130.7, 128.7, 128.3, 127.8, 127.8, 127.3, 126.5, 113.1, 112.9, 112.2, 112.1, 102.8, 102.6, 102.4. ^{19}F NMR (470 MHz, DMSO-d_6) δ -118.4 (s), -119.5 (s).

HRMS (ESI$^+$): *m/z* calcd. for $C_{12}H_8ClFN_2O_2S$ [*M*–H]$^-$ 296.9906, measured 296.99024.

(*E*)-5-Chloro-*N*'-((6-(trifluoromethyl)pyridin-3-yl)methylene)thiophene-2-carbohydrazide (A2H5)

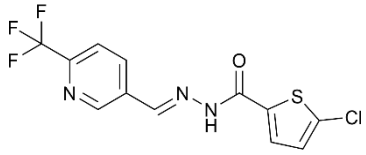

According to GP-3, 6-(trifluoromethyl)nicotinaldehyde **A2** (60 mg, 0.34 mmol) and 5-chlorothiophene-2-carbohydrazide **H5** (60.52 mg, 0.34 mmol) were mixed in MeOH(0.52 mL). The crude was purified by preparative HPLC (70% CH_3CN) to afford **A2H5** as a mixture of two rotamers of the amide CO–NH (73:27) as a white solid (102 mg, 0.34 mmol, 89%). ^{1}H NMR (500 MHz, DMSO-d_6) δ 12.34 (br. s, 2H, 1Ha and 1Ha'), 9.18 – 9.00 (m, 2H, 1Ha and 1Ha'), 8.48 – 8.35 (m, J = 7.5 Hz, 3H, 1Ha and 2Ha'), 8.24 (s, 1H, Ha), 8.13 – 8.02 (m, J = 7.9 Hz, 2H, 1Ha and 1Ha'), 7.83 (s, 2H, 1Ha and 1Ha'), 7.29 (d, J = 4.1 Hz, 2H, 1Ha and 1Ha'). ^{13}C NMR (126 MHz, DMSO-d_6) δ 160.8, 149.4, 147.2, 147.2, 147.2, 146.9, 146.9, 146.9, 144.1, 144.0, 144.0, 141.2, 141.1, 138.1, 136.6, 136.1, 135.4, 133.6, 130.5, 130.0, 129.9, 129.9, 128.9, 128.9, 128.8, 127.2, 123.1, 121.70, 120.98, 120.95, 120.93. ^{19}F NMR (470 MHz, DMSO-d_6) δ –66.4, –66.5.

HRMS (ESI$^+$): *m/z* calcd. for $C_{12}H_7ClF_3N_3OS$ [*M*-H]$^-$ 331.98777, measured 331.98724.

(*E*)-*N*'-(2-Fluoro-4-hydroxybenzylidene)-2-(4-nitrophenoxy)acetohydrazide (A1H6)

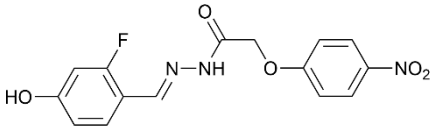

According to GP-3, 2-fluoro-4-hydroxybenzaldehyde **A1** (40 mg, 0.286 mmol) and 2-(4-nitrophenoxy)acetohydrazide **H6** (60.3 mg, 0.286 mmol) were mixed in MeOH (0.48 mL). The crude was purified by preparative HPLC (60% CH_3CN) to afford **A1H6** as a mixture of two rotamers of the amide CO–NH (70:30) as a white solid (76 mg, 0.286 mmol, 80%).

^{1}H NMR (500 MHz, DMSO-d_6) δ 11.59 (d, J = 13.1 Hz, 2H, 1Ha and 1Ha'), 10.48 (s, 2H, 1Ha and 1Ha'), 8.43 (s, 1H, Ha'), 8.24 (d, J = 9.2 Hz, 2H, Ha'), 8.20 (d, 9H), 8.11 (s, 5H), 7.77 (t, J = 8.7 Hz, 2H, 1Ha and 1Ha'), 7.71 (t, J = 8.7 Hz, 1H, Ha'), 7.20 (d, J = 9.3 Hz, 2H, Ha'), 7.17 – 7.09 (m, 10H), 6.70 (dd, J = 8.6, 2.2 Hz, 7H), 6.62 (dd, J = 12.7, 2.2 Hz, 7H), 5.31 (s, 2H, Ha), 4.83 (s, 2H, Ha'). ^{13}C NMR (126 MHz, DMSO-d_6) δ 167.9, 163.6, 163.1, 163.0, 162.9, 162.7, 161.0, 160.9, 160.7, 141.3, 141.3, 140.9, 137.5, 137.5, 127.5, 127.5, 127.4, 127.4, 125.8, 125.7, 115.3, 115.2, 112.8, 112.7, 112.3, 112.3, 102.6, 102.6, 102.4, 102.4, 66.7, 65.4. ^{19}F NMR (470 MHz, DMSO-d_6) δ −119.45, −119.69.

HRMS (ESI$^+$): *m/z* calcd. for $C_{15}H_{12}FN_3O_5$ [*M*+H]$^+$ 332.06882, measured 332.06827.

(*E*)-*N*'-(2-Fluoro-4-hydroxybenzylidene)thiophene-2-carbohydrazide (A1H7)

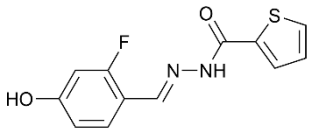

According to GP-3, 2-fluoro-4-hydroxybenzaldehyde **A1** (50 mg, 0.36 mmol) and thiophene-2-carbohydrazide **H7** (50.7 mg, 0.36 mmol) were mixed in MeOH (0.6 mL). The crude was purified by preparative HPLC (50% CH_3CN) to afford **A1H7** as a mixture of two rotamers of the amide CO–NH (51:49) as a white solid (87 mg, 0.36 mmol, 90%).

1H NMR (500 MHz, DMSO-d_6) δ 11.78 (d, 2H, 1Ha and 1Ha'), 10.48 (s, 2H, 1Ha and 1Ha'), 8.55 (s, 1, Ha'), 8.21 (s, 1H, 1Ha), 8.04 (s, 1H, Ha), 7.98 – 7.64 (m, 4H, 2Ha and 2Ha'), 7.22 (t, J = 4.2 Hz, 2H, 1Ha and 1Ha'), 6.75 (dd, J = 21.3, 8.1 Hz, 2H, 1Ha and 1Ha'), 6.64 (d, J = 12.5 Hz, 2H, 1Ha and 1 Ha'). ^{13}C NMR (126 MHz, DMSO-d_6) δ 162.86, 161.09, 160.94, 160.87, 157.51, 157.5, ^{14}0.7, 138.3, 137.4, 134.8, 134.6, 133.2, 131.8, 128.8, 128.14, 127.7, 127.6, 127.3, 126.7, 113.0, 112.8, 112.7, 112.6, 112.5, 102.7, 102.6, 102.5, 102.4. ^{19}F NMR (470 MHz, DMSO-d_6) δ -118.3 (s), -119.4 (s).

HRMS (ESI+): m/z calcd. for $C_{12}H_{18}FN_2O_2S$ [M−H]− 263.02960, measured 263.02908.

.

(***E*)-4-Methyl-*N*'-((6-methylpyridin-3-yl)methylene)benzenesulfonohydrazide (A3H8)**

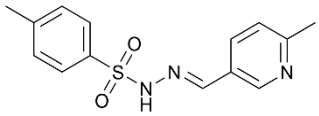

According to GP-, 6-methylnicotinaldehyde **A3** (80 mg, 0.66 mmol) and 4-methylbenzenesulfonohydrazide **H8** (112.42 mg, 0.34 mmol) were mixed in MeOH (1.1 mL) to afford after purification by preparative HPLC (50% CH_3CN) **A3H8** as one rotamer of the amide CO–NH) as a yellow solid (183.23 mg, 0.66 mmol, 96%).

^{1}H NMR (500 MHz, DMSO-d_6) δ 11.75 (s, 1H), 8.82 (s, 2H), 7.90 (s, 1H), 7.77 (d, J = 8.2 Hz, 2H), 7.41 (d, J = 8.1 Hz, 2H), 2.61 (s, 3H), 2.36 (s, 3H). ^{13}C NMR (126 MHz, DMSO-d_6) δ 168.0, 154.8, 143.6, 141.7, 135.9, 129.7, 127.3, 124.8, 25.6, 21.0.

HRMS (ESI$^+$): *m/z* calcd. for $C_{14}H_{15}N_3O_2S$ [*M*+H]$^+$ 291.09913, measured 291.08968.

(*E*)-5-((2-(1-Naphthoyl)hydrazineylidene)methyl)-2-hydroxybenzoic acid (3, **A4H9**)

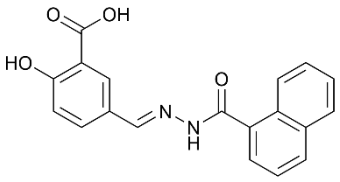

According to GP-3, 5-formyl-2-hydroxybenzoic acid, **A4** (100 mg, 0.602 mmol) and 1-naphthohydrazide **H9** (112.09 mg, 0.602 mmol) were mixed in MeOH (1.1 mL) to afford after preparative HPLC (70% CH_3CN) (*E*)-5-((2-(1-Naphthoyl)hydrazineylidene)methyl)-2-hydroxybenzoic acid **3** (**A4H9**) as a mixture of two rotamers of the amide CO–NH (84:16) as an off-white solid (105 mg, 0.602 mmol, 92%).

^{1}H NMR (500 MHz, DMSO-d_6) δ 11.96 (s, 2H, Ha and Ha'), 8.29 (s, 1H), 8.23 – 8.18 (m, J = 6.4, 2.8 Hz, 1H, Ha), 8.16 (d, J = 2.2 Hz, 1H, Ha), 8.09 (d, J = 8.2 Hz, 1H, Ha), 8.05 – 7.98 (m, 4H, 1Ha and 3Ha'), 7.90 (dd, J = 14.3, 7.1 Hz, 2H, 1Ha and 1Ha'), 7.74 (dd, 1H, Ha), 7.69 (d, 1H, Ha'), 7.64 – 7.50 (m, 6H, 3Ha and 3Ha'), 7.29 (dd, J = 8.7 Hz, 1H, Ha'), 7.07 (d, J = 8.6 Hz, 1H, Ha), 6.83 (d, J = 8.6 Hz, 1H, Ha'). ^{13}C NMR (126 MHz, DMSO-d_6) δ 171.4, 164.6, 163.0, 147.0, 133.4, 133.2, 133.0, 130.4, 130.0, 129.4, 128.4, 127.1, 126.5, 125.8, 125.2, 125.0, 117.9.

HRMS (ESI$^+$): m/z calcd. for $C_{19}H_{14}N_2O_4$ [*M*+H]$^+$ 335.10263, measured 335.1007.

(*E*)-4-Bromo-*N*'-((5-(4-chlorophenyl)furan-3-yl)methylene)benzohydrazide (4, A5H10)

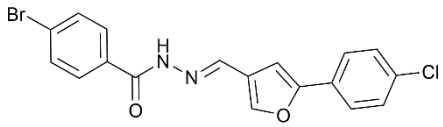

According to GP-3, 5-(4-chlorophenyl)furan-3-carbaldehyde **A5** (40 mg, 0.19 mmol) and 4-bromobenzohydrazide **H10** (41.63 mg, 0.19 mmol) were mixed in MeOH (0.32 mL) to give after purification by preparative HPLC (80% CH_3CN) **4 (A5H10)** as a mixture of two rotamers of the amide CO–NH (91:9) as a yellow solid (59.2 mg, 0.194 mmol, 76%).

^{1}H NMR (500 MHz, DMSO-d_6) δ 11.93 (brs, 2H, 1Ha and 1Ha'), 8.37 (s, 1H), 7.93 – 7.70 (m, 12H, 6Ha and Ha'), 7.54 (d, J = 8.4 Hz, 4H, 2Ha and 2Ha'), 7.15 (dd, J = 58.7, 3.2 Hz, 4H, 2Ha and 2Ha'). ^{13}C NMR (126 MHz, DMSO-d_6) δ 162.1, 153.7, 149.3, 137.5, 132.7, 132.4, 131.5, 129.7, 129.1, 128.3, 125.7, 125.6, 116.4, 109.1.

HRMS (ESI$^+$): *m/z* calcd. for $C_{18}H_{12}BrClN_2O_2$ [*M*+H]$^+$ 404.98230, measured 404.98146.

(*E*)-*N*'-((5-(4-Chlorophenyl)furan-2-yl)methylene)-1-naphthohydrazide (5, A5H9)

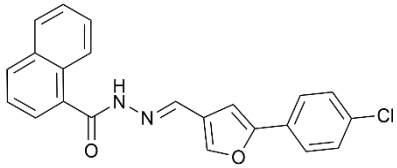

According to GP-3, 5-(4-chlorophenyl)furan-3-carbaldehyde **A5** (100 mg, 0.48 mmol) and 1-naphthohydrazide **H9** (90.1 mg, 0.48 mmol) were mixed in MeOH (0.8 mL). The crude was purified by preparative HPLC (84% CH_3CN) to afford **(A5H9)** as a mixture of two rotamers of the amide CO–NH (89:11) as a yellow solid (136mg, 0.64 mmol, 75%).

^{1}H NMR (500 MHz, DMSO-d_6) δ 12.07 – 11.97 (m, 2H, 1Ha and 1Ha'), 8.25 (s, 1H), 8.23 – 8.19 (m, 1Ha), 8.18 – 8.06 (m, 3H, 1Ha and 2Ha'), 8.03 (dd, 3H, 1Ha and 2 Ha'), 7.91 (td, J = 16.2, 7.4 Hz, 2H, Ha'), 7.84 (d, J = 8.5 Hz, 2H, Ha), 7.75 (d, J = 6.9 Hz, 1H, Ha), 7.64 – 7.59 (m, 6H, 3Ha and 3Ha'), 7.55 (d, J = 8.5 Hz, 4H, 2Ha and 2Ha'), 7.22 (d, J = 3.6 Hz, 1H, Ha), 7.09 (d, J = 3.6 Hz, 1H, Ha), 7.02 (d, 1H, Ha'), 6.72 (d, 1H, Ha'). ^{13}C NMR (126 MHz, DMSO-d_6) δ 164.6, 153.7, 149.3, 137.1, 133.2, 132.8, 132.7, 130.6, 129.9, 129.16, 128.4, 127.2, 126.5, 125.9, 125.7, 125.0, 125.0, 116.3, 109.1.

HRMS (ESI$^+$): m/z calcd. for $C_{22}H_{15}ClN_2O_2$ [*M*+H]$^+$ 375.08948, measured 375.0890.

5-((*E*)-(2-(2-((3*R*,5*R*,7*R*)-adamantan-1-yl)acetyl)hydrazineylidene)methyl)-2-hydroxybenzamide (6, A6H19)

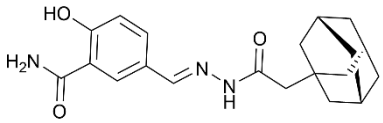

According to GP-3, 5-formyl-2-hydroxybenzamide **A6** (50 mg, 0.30 mmol) and adamantane-1-yl-acetic acid hydrazide **H19** (67.3 mg, 0.30 mmol) were mixed in MeOH (0.5 mL). The crude was purified by preparative HPLC (75% CH_3CN) to afford **6** (**A6H19)** as a mixture of two rotamers of the amide CO–NH (57:43) as an off-white solid (78 mg, 0.3 mmol, 72%).

^{1}H NMR (500 MHz, DMSO-d_6) δ 13.29 (s, 2H, 1Ha and 1Ha'), 11.16 (d, J = 10.8 Hz, 2H, 1Ha and 1Ha'), 8.53 (d, J = 9.3 Hz, 2H, 1Ha and 1 Ha'), 8.09 (s, 1H), 8.04 (dd, J = 27.2, 1.6 Hz, 1H), 7.99 (s, 1H), 7.87 (s, 1H), 7.78 (ddd, J = 18.4, 8.7, 1.7 Hz, 2H, 1Ha and 1Ha'), 6.96 (t, J = 9.2 Hz, 2H, 1Ha and 1Ha'), 1.92 (d, J = 15.7 Hz, 8H), 1.74 – 1.42 (m, 25H).

^{13}C NMR (126 MHz, DMSO-d_6) δ 172.6, 172.0, 171.9, 166.6, 162.8, 145.5, 141.5, 132.1, 131.0, 128.8, 128.5, 125.7, 125.6, 119.0, 118.6, 115.8, 115.2, 115.2, 114.9, 49.1, 45.3, 42.9, 42.6, 36.9, 33.4, 33.2, 28.5.

HRMS (ESI$^+$): m/z calcd. for $C_{20}H_{25}N_3O_3$ [*M*+H]$^+$ 356.19687, measured 356.19603.

(*E*)-*N*'-((6-(Benzyloxy)-1*H*-indol-3-yl)methylene)-2-(naphthalen-1-yloxy)acetohydrazide (A7H15)

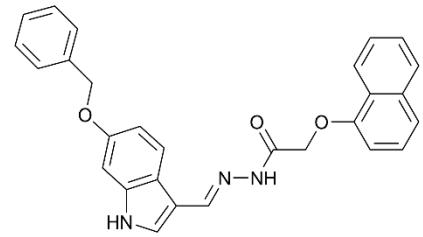

According to GP-3, 6-(benzyloxy)-1H-indole-3-carbaldehyde **A7** (50 mg, 0.2 mmol) and 2-(naphthalen-1-yloxy)acetohydrazide **H15** (172 mg, 0.8 mmol) were mixed in MeOH (0.33 mL) to give after purification by preparative HPLC (78% CH_3CN) **A7H15** as a mixture of two rotamers of the amide CO–NH (67:33) as an off-white solid (63 mg, 0.2 mmol, 70%).

^{1}H NMR (500 MHz, DMSO-d_6) δ 11.41 (s, 2H, 1Ha and Ha'), 11.38 (s, 1H, Ha), 11.34 (s, 1H, Ha'), 8.43 (s, 1H, Ha'), 8.37 – 8.31 (m, 1H, Ha'), 8.30 – 8.25 (m, 1H, Ha), 8.16 (s, 1H, Ha), 8.09 (d, J = 8.7 Hz, 1H, Ha'), 8.01 (d, J = 8.7 Hz, 1H, Ha), 7.92 – 7.86 (m, 2H, 1Ha and 1Ha'), 7.69 (dd, J = 7.5, 2.6 Hz, 2H, 1Ha and 1Ha'), 7.59 – 7.36 (m, 14H, 7Ha and 5Ha'), 7.32 (dt, J = 11.8, 5.8 Hz, 2H, 1Ha and 1Ha'), 7.00 (d, J = 1.8 Hz, 2H, 1Ha and 1Ha'), 6.97 (d, J = 7.6 Hz, 1H, Ha'), 6.92 – 6.85 (m, 3H, 1Ha and 2Ha'), 6.85 (d, J = 2.2 Hz, 1H,

Ha'), 5.39 (s, 2H, Ha), 5.13 (s, 3H, 2Ha and 1Ha'), 4.84 (s, 2H, Ha'). ^{13}C NMR (126 MHz, DMSO-d_6) δ 168.40, 155.8, 155.8, 154.26, 154.0, 145.6, 141.8, 138.3, 138.2, 137.9, 134.6, 134.6, 130.2, 128.9, 128.2, 128.1, 128.0, 127.9, 127.0, 126.9, 126.6, 126.5, 125.8, 125.7, 125.4, 125.4, 123.0, 122.8, 122.5, 122.2, 121.1, 120.6, 119.1, 118.9, 112.0, 111.9, 111.6, 111.4, 106.1, 105.7, 96.8, 96.7, 69.9, 69.9, 67.6, 65.7.
HRMS (ESI$^+$): m/z calcd. for $C_{28}H_{23}N_3O_3$ [*M*+H]$^+$ 450.18122, measured 450.18049.

2-((3*R*,5*R*,7*R*)-Adamantan-1-yl)-*N*'-((E)-(6-(benzyloxy)-1H-indol-3-yl)methylene)acetohydrazide (A7H19)

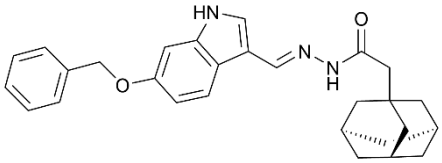

According to GP-3, 6-(benzyloxy)-1H-indole-3-carbaldehyde **A7** (50 mg, 0.2 mmol) and adamantane-1-yl-acetic acid hydrazide **H19** (41.45 mg, 0.2 mmol). Were mixed in MeOH (0.33 mL). The crude was purified by preparative HPLC (80% CH_3CN) to afford **A7H19** as a mixture of two rotamers of the amide CO–NH (46:44) as a yellow solid (80 mg, 0.24 mmol, 77%).
^{1}H NMR (500 MHz, DMSO-d_6)) δ 11.29 (dd, *J* = 12.8, 2.0 Hz, 2H, 1Ha and 1Ha'), 8.88 (s, 2H, 1Ha and 1Ha'), 8.25 (s, 1H), 8.06 (dd, *J* = 12.9, 8.6 Hz, 3H, 2Ha and 1Ha'), 7.56 (dt, *J* = 17.3, 8.6 Hz, 2H, 1Ha and 1Ha'), 7.45 (dt, *J* = 15.4, 7.8 Hz, 4H, 2Ha and 2Ha'), 7.38 (td, *J* = 7.5, 1.8 Hz, 4H, 2Ha and 2Ha'), 7.34 – 7.28 (m, 2H, 1Ha and 1Ha'), 7.00 (dd, *J* = 6.5, 2.2 Hz, 2H, 1Ha and 1Ha'), 6.86 (ddd, *J* = 13.0, 8.7, 2.2 Hz, 2H, 1Ha and 1Ha'), 5.12 (d, *J* = 5.7 Hz, 4H, 2Ha and 2Ha'), 1.94 – 1.85 (m, 5H), 1.53 (t, *J* = 10.2 Hz, 47H). ^{13}C NMR (126 MHz, DMSO-d_6) δ 172.14, 170.09, 155.72, 143.32, 139.80, 138.30, 138.18, 137.83, 137.82, 129.47, 129.37, 128.88, 128.20, 128.08, 128.00, 123.08, 122.41, 121.38, 119.06, 118.92, 112.20, 111.24, 96.98, 96.88, 96.65, 69.93, 48.35, 42.97, 42.48, 36.85, 33.57, 33.09, 32.59, 28.46.
HRMS (ESI$^+$): m/z calcd. for $C_{28}H_{31}N_3O_2$ [M+H]$^+$ 442.24890, measured 442.24831.

Biological evaluation of synthesized compounds

Protein homology sequence and structure identity determination of the entire complex of ECF-PanT

The NCBI BLAST program was utilized to conduct the BLAST analysis with specific parameters, including BLASTp and an E-value threshold of 0.05. The query protein under examination was *S. pneumoniae* ECF-PanT with UniProtKB database ID of EcfS: A0A064C5C4, EcfT: A0A4L7ULF4, EcfA1: Q04HV7, and EcfA2: Q97N51, while the subject protein was *L. delbrueckii* ECF PanT with PDB ID of 6ZG3 and UniProtKB ID of EcfS: Q1GBG0, EcfT: Q1GBI8, EcfA1: Q1GBJ0, and EcfA2: Q1GBI9. The resulting values obtained from the analysis were an E-value of 0 and a percentage identity of 40.80 %.[6, 7]

In this study, the multiple sequence alignment with both the query and subject proteins was produced by T-Coffee[8,9] and nimBOXshade was utilized to enhance the presentation of the sequence alignments in shade (Figure S4).[10]

```
S.ECF-PanT     1 MK------KRSNIAPIAIFFATMLVIHFLSSLIFNLFPFPIKPTIVHIPVIIA--SIIYG
L.ECF-PanT     1 MYDSEARQKTLNLTVSAVFVAILLLEAFIPNVGY-ITILPGLPAITTIPLTVAVFASLRG

                   ....:...70....:...80....:...90....:..100....:..110....:..120
S.ECF-PanT    53 PRVGVTLGFLMGLLSLTVNTITILPTSYLFSPFVPNGNI-----YSAIIAIVPRILIGLT
L.ECF-PanT    60 PKAGAAFGLVWGLTSLLRA------------YVAPNGLVTILLFQNPLIALLPRLAAGWA

                   ....:..130....:..140....:..150....:..160....:..170....:..180
S.ECF-PanT   108 PYLVYKLM-------KNKTGLILAGALGSLTNTIFVLG-----------GIFFLFGNVYN
L.ECF-PanT   108 AGLAGQLADKWEKESRKPLAYALSGLLASAVNTLIVILLSDLVYFIHPQKLALALGAKSG

                   ....:..190....:..200....:..210....:..220....:..230....:..240
S.ECF-PanT   150 GNIQLLLATVISTNSIAELVISAILTLAIVP-RLQTL-KKMDSMILGRYIPGDSIVHRLD
L.ECF-PanT   168 QSLLVILFTALAVNGILEAVFSGLITPLITAPLKKRLKRRMSKIIIGRYLPGTTFVYRVD

                   ....:..250....:..260....:..270....:..280....:..290....:..300
S.ECF-PanT   208 PRSKLLAMMLLILIVFWANNPLTNLILFIATGIFIALSGVSLSFFIQGLKSIFFLIAFTT
L.ECF-PanT   228 PRAKLLTTFYFIIMIFLANNWVSYLVISIFGLAYVFATGLKARVFWDGVKPMIWMIVFTS

                   ....:..310....:..320....:..330....:..340....:..350....:..360
S.ECF-PanT   268 IFQLFFISNGNVLFEFSFVRITDYALQQAGIIFCRFVLIIFFSTLLTLTTMPLSLASAVE
L.ECF-PanT   288 LLQTFFMAGGKVYWHWWIFTLSSEGLINGLYVFIRFAMIILVSTVMTVTTKPLEIADAME

                   ....:..370....:..380....:..390....:..400....:..410....:..420
S.ECF-PanT   328 ALLAPLKRVKVPVHEIGLMLSMSLRFVPTLMDDTTRIMNAQKARGVDFGEGSIVQKVKAM
L.ECF-PanT   348 WMLTPLKLFKVNVGMISLVISIALRFVPTLFDQTVKIMNAQRSRGADFNDGGLVKRAKSV

                   ....:..430....:..440....:..450....:..460....:..470....:..480
S.ECF-PanT   388 IPILIPLFATSLKRADSLAIAMEARGYQGGKGRSQYRQLKWTLKDTLTILVILVLGCCLF
L.ECF-PanT   408 VPMLVPLFIDSLEVALDLSTAMESRGYKGSEGRTRYRILEWSKVDLIPVAYCLLLTILMI

                   ....:..490....:..500....:..510....:..520....:..530....:..540
S.ECF-PanT   448 -FLKSMGIALENVNFTYQEGTPLASAALSDVSLTIEDGSYTALIGHTGSGKSTILQLLNG
L.ECF-PanT   468 TTRKHMAIKFENVSYVYSPGSPLEAIGLDQLNFSLEEGKFIALVGHTGSGKSTLMQHFNA

                   ....:..550....:..560....:..570....:..580....:..590....:..600
S.ECF-PanT   507 LLVPSQGSVRVFDTLITSTSKNKDIRQIRKQVGLVFQFAENQIFEETVLKDVAFGPQNFG
L.ECF-PanT   528 LLKPTSGKIEIAGYTITPETGNKGLKDLRRKVSLAFQFSEAQLFENTVLKDVEYGPRNFG

                   ....:..610....:..620....:..630....:..640....:..650....:..660
S.ECF-PanT   567 VSEEDAVKTAREKLALVGIDESLFDRSPFELSGGQMRRVAIAGILAMEPAILVLDEPTAG
L.ECF-PanT   588 FSEDEAREAALKWLKKVGLKDDLIEHSPFDLSGGQMRRVALAGVLAYEPEIICLDEPAAG

                   ....:..670....:..680....:..690....:..700....:..710....:..720
S.ECF-PanT   627 LDPLGRKELMTLFKKLHQSGMTIVLVTHLMDDVAEYANQVYVMEKGRLVKGGKPSDVFQD
L.ECF-PanT   648 LDPMGRLEMMQLFKDYQAAGHTVILVTHNMDDVADYADDVLALEHGRLIKHASPKEVFKD

                   ....:..730....:..740....:..750....:..760....:..770....:..780
S.ECF-PanT   687 VVFMEEVQLGVPKITAFCKRLADRGVSFKRLPIKIEEFKE----SLNGM-----KSIIDV
L.ECF-PanT   708 SEWLQKHHLAEPRSARFAAKLEAAGLKLPGQPLTMPELADAIKQSLKGGEHEMSDNIISF

                   ....:..790....:..800....:..810....:..820....:..830....:..840
S.ECF-PanT   738 KNLSFRYKENQNYYDVKDITFHVKRGEWLSIVGHNGSGKSTTVRLIDGLLEA---ESGEI
L.ECF-PanT   768 DHVTFTYPDSPR-PALSDLSFAIERGSWTALIGHNGSGKSTVSKLINGLLAPDDLDKSSI

                   ....:..850....:..860....:..870....:..880....:..890....:..900
S.ECF-PanT   795 VIDGQRLTEENVWNIRRQIGMVFQNPDNQFVGATVEDDVAFGLENQGLSRQEMKKRVEEA
L.ECF-PanT   827 TVDGVKLGADTVWEVREKVGIVFQNPDNQFVGATVSDDVAFGLENRAVPRPEMLKIVAQA

                   ....:..910....:..920....:..930....:..940....:..950....:..960
S.ECF-PanT   855 LALVGMLDFKKREPARLSGGQKQRVAIAGVVALRPAILILDEATSMLDPEGRRELIGTVK
L.ECF-PanT   887 VADVGMADYADSEPSNLSGGQKQRVAIAGILAVKPQVIILDESTSMLDPEGKEQILDLVR

                   ....:..970....:..980....:..990....:.1000....:.1010....:.1020
S.ECF-PanT   915 GIRKDYDMTVISITHDLEEVAMSDRVLVMKKGEIESTSSPRELFSRND-LDQIGLDDPFA
L.ECF-PanT   947 KIKEDNNLTVISITHDLEEAAGADQVLVLDDGQLLDQGKPEEIFPKVEMLKRIGLDIPFV
```

```
                ....:.1030....:.1040....:.1050....:
S.ECF-PanT   974 NQLKKSLSQNGYDLPENYLTESELEDKLWELL---
L.ECF-PanT  1007 YRLKQLLKERGIVLPDEIDDDEKLVQSLWQLNSKM
```

Figure S4. The fraction of sequences that must agree for a consensus (0–1) was set to 0.5. The foreground color for both identical and similar residues was set to black. The background color for identical and similar residues was set to green and yellow, respectively.

Uptake assay into proteoliposome

To assess the effectiveness of the tDCC compounds inhibiting the ECF proteins, we performed an uptake assay inspired by Swier *et al*.[11] In this assay, the ECF transporter for folate (ECF-FolT2) from *L. delbrueckii* was used and reconstituted into lipid vesicles known as proteoliposomes. For our purposes, we utilized the ECF transporter for pantothenate (ECF-PanT) from *L. delbrueckii*. This choice was made for two reasons: firstly, it originates from the same organism for which the assay was initially designed, and secondly, it exhibits homology to *S. pneumoniae* ECF-PanT as confirmed through BLASTp analysis (Figure S4), demonstrating a sufficient sequence similarity of 34%. This similarity allows us to use *L. delbrueckii* ECF-PanT as a representative model, enabling meaningful comparisons and insights applicable to both proteins and their respective organisms. Figure S5 exhibits the percentage of inhibition for each compound at 250 µM. In Figures S6A and S6B, pantothenate uptake traces are shown. Mg-ATP and Mg-ADP were used as positive and negative controls, respectively. The differences in the uptake patterns for the 5 mM Mg-ATP control can be explained by how recently we purified the protein, as over time, the protein tends to lose its activity.

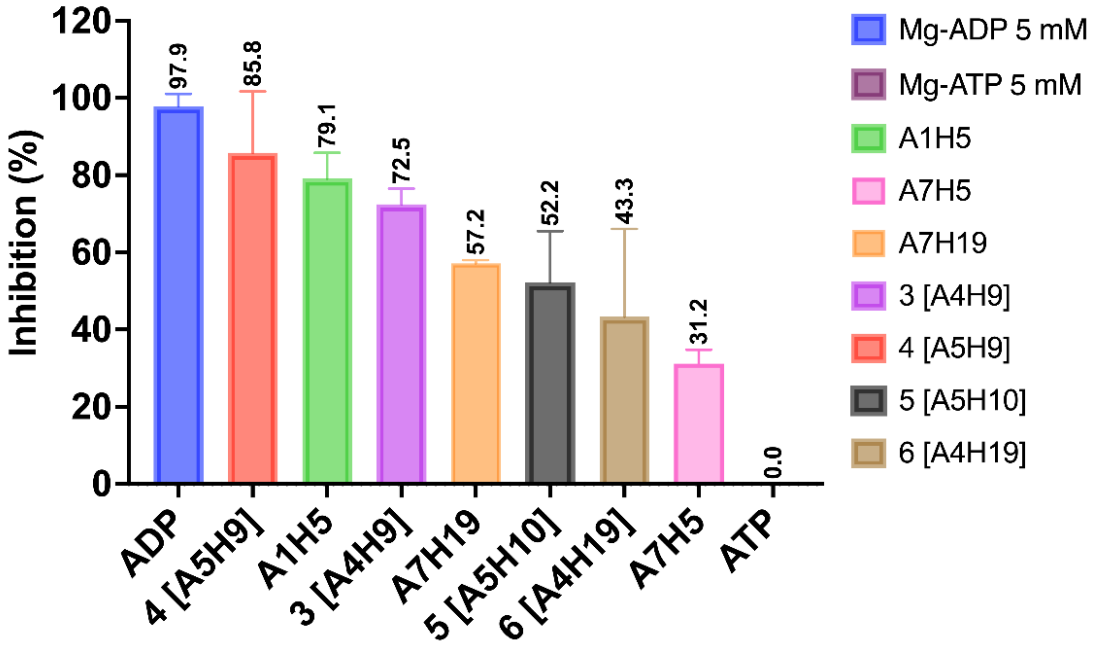

Figure S5. The graph displays inhibition percentages for individual target-directed combinatorial chemistry (td-DCC) product compounds at a concentration of 250 µM, obtained through the proteoliposome uptake assay, and is presented in column format.

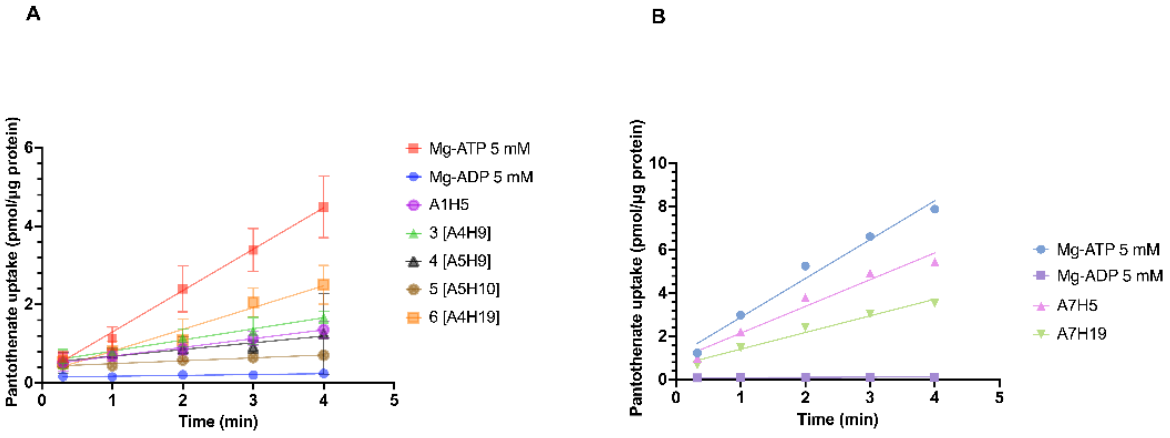

Figure S6. A and B both show the pantothenate uptake traces for Lactobacillus delbrueckii ECF-PanT protein reconstituted in a 1:125 ratio. The corresponding line for each compound is between Mg-ATP as a positive control and Mg-ADP as a negative control. Figure 6. A depicts the results of the assay conducted with three technical replicates, each of which was performed as a duplicate biological assay. Figure 6. B illustrates the results obtained from a single biological and technical replicate assay.Whole-cell bacterial uptake assay (ECF-T assay)

The ECF inhibitors and their inhibitory effect on folate uptake in the Gram-positive model organism *L. casei* were studied in a whole-cell uptake assay as recently published in our group.[12] For this purpose, 20 µL of inhibitor, was added to the wells of a MultiScreen HTS Filter Plate containing 175 µL of *L. casei* culture diluted in citrate buffer. The blank was determined with 185 µL citrate buffer and 10 µL of DMSO. 5 µL of radiolabeled folic acid was added to each well (2 µM, Moravek Biochemicals, Brea, CA). Using this method, we determined the percentage of inhibition at 200 µM for the building blocks and the amplified compounds (Figure S7) and the IC_{50} values for our best compounds. The assay was done in both technical and biological duplicate ensuring the reliability and consistency of the data. Subsequently, the gathered data were analyzed using GraphPad Prism, a robust statistical software tool.

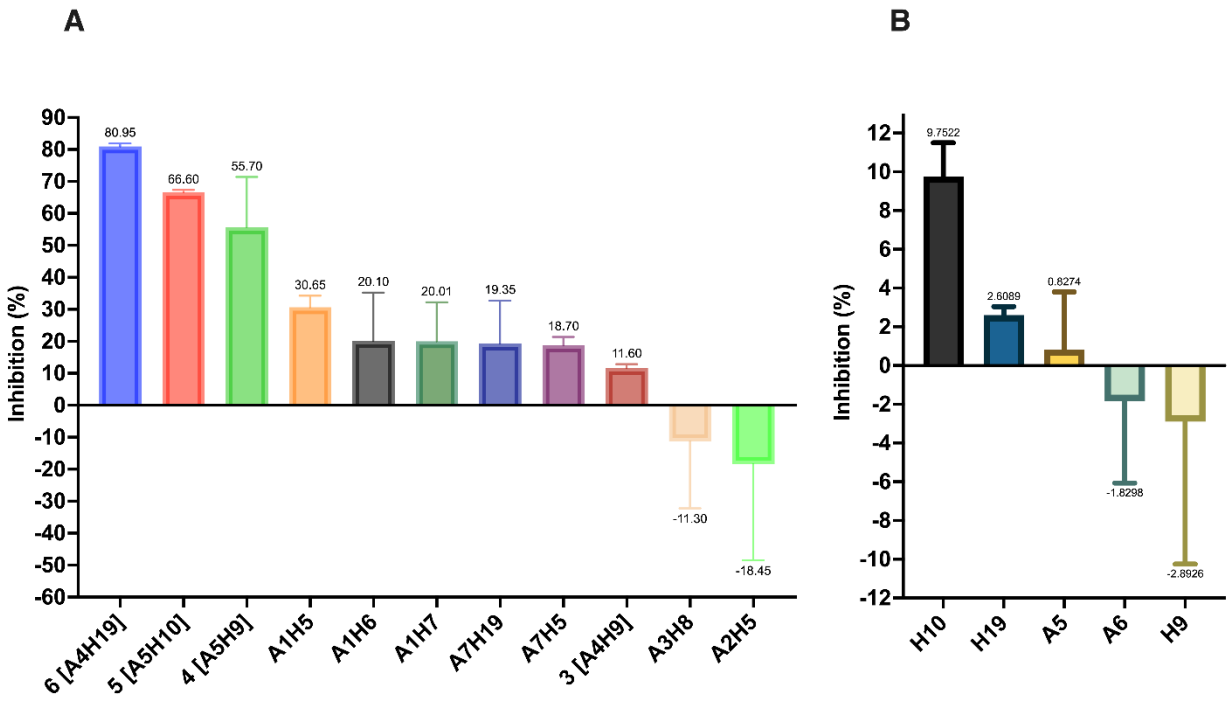

Figure S7. The figure depicts the percentage of inhibition of **A)** target-directed combinatorial chemistry (tdDCC) product compounds and **B)** building blocks at a concentration of 200 µM, as determined through the whole-cell-based uptake assay.

Cytotoxicity assays

To obtain information regarding the cytotoxicity of our compounds, their impact on the viability of human cells was investigated. HepG2, HEK293 and A549 cells (2x10^5 cells per well) were seeded in 24-well, flat-bottomed culture plates. Twenty-four hours after seeding the cells, the incubation was started by the addition of compounds in a final DMSO concentration of 1%. Duplicates were prepared for each compound concentration. Epirubicin and doxorubicin were used as positive controls (each at 1 µM), and rifampicin was used as a negative control (at 100 µM). The living cell mass was determined 48 h after treatment with compounds by adding 0.1 volumes of 3-(4,5-dimethylthiazol-2-yl)-2,5-diphenyltetrazolium bromide (MTT) solution (5 mg per mL sterile PBS) (Sigma, St. Louis, MO) to the wells. After incubating the cells at 37 °C for 30 min (atmosphere containing 5% CO2), MTT crystals were dissolved in a solution containing 10% SDS and 0.5% acetic acid in DMSO. The optical density (OD) of the samples was determined photometrically at 570 nm in a FLUOstar Omega plate reader (BMG labtech, Ortenberg, Germany). To obtain percent inhibition values for each sample, their ODs were related to those of DMSO controls. At least two independent measurements were performed for each compound.[13]

Table 4. Antibacterial activity and cytotoxicity results for compounds **4**, **5** and **6** in three different cell lines.

Compound	Cytotoxicity % Inh. @ 100 µM			Antibacterial profile (µM)	
	HepG2	A549	HEK293	*Streptococcus pneumoniae* DSM-20566	*Streptococcus pneumoniae* DSM-11865 (PRSP)
4	<10	<10	<10	>64	>64
5	<10	<10	<10	>64	>64
6	<10	20 ± 3	<10	>64	>64

Computational Modeling

Methods:

Data sets: From the coarse-grained MD simulation of *L. delbrueckii* ECF-PanT transporter X-ray crystal structure (PDB ID: 6ZG3) with hit compound **1**, two snapshots with the best calculated free energies were selected.[14] These snapshots provided two distinct binding pockets, P11, a cavity in the S-component, and P9, a hidden pocket at the interface between ECF-T and the S-component, as described in Diamanti *et al.*[14] Three potent inhibitors, two compounds from the hit **2** series (**4** and **5**) and compound **6** from the hit **1** series, were chosen to examine the binding mode commonalities and differences between both different hit series. Distinct isomers were used as input for the docking study for compounds that contain an acylhydrazone moiety (**4**, **5** and **6**) to be able to pick the enantiomer that fits better to the binding site for the downstream studies.

Docking: As in the previous study,[14] we used FlexX for protein–ligand docking from SeeSAR version 13.0.1[15] to generate docking poses for the selected three compounds. The CG-MD snapshot with hit1 compound bound to pocket P9 was used as input, and the bound ligand, **1**, served to define the binding site. Thirty poses for every compound were generated using the default parameters. All poses were evaluated using the built-in HYDE scoring function.[16]

Manual pose selection: We selected poses with favorable estimated affinity that mimic the key interactions of hit compound **1**, contained in pocket P9 in the CG-MD snapshot. Thus, for **6**, the pose was chosen that most closely overlapped with the salicylic acid moiety of **1**. In both series, poses forming hydrogen-bond interactions with the side chain of ARG77-C were preferred. Note that for **4**, **5** and **6** the *E*-enantiomers were selected for analysis and for MD simulations due to their better fit.
MD Simulations: MD simulations were performed to answer different questions, the general set-up has been the same, only the chosen poses differ.
First, the protein structure was prepared using PDBFixer from OpenMM.[17] Missing hydrogen atoms were added, and missing residues were ignored. Selected poses were prepared using RDKit[18] to protonate the compounds and to assign the bond order correctly. The system was then prepared for the MD simulations: Parameters for the protein were generated from the amber14-all force field within OpenMM; for the compound parameters, we used the General AMBER Force Field (GAFF).[19] The complex was embedded in a cubic box, the dimensions of the box were set based on the largest dimension of the complex, including padding. The system has been solvated using the standard three-site water model TIP3P.[20] Langevin integrator[21] was the method of choice for simulating the created system by integrating the equations of motion. The starting position was set by minimizing the energy of the system first to decrease the probability of simulation failures. We simulated 60 picoseconds of MD corresponding to 30,000 steps of 2 femtosecond each. Snapshots were saved every 2000 steps (4 picoseconds), having 150 snapshots at the end of each MD simulation.
I) MD simulations to select pocket: To confirm the selected binding pocket, we performed an MD simulation using the three potent compounds (**4**, **5** and **6**) for both binding pockets P11 and P9. The highest-scoring poses were selected for each binding pocket from the FlexX docking using HYDE scoring function (see docking section).
II) MD simulations to test stability: To support the docking hypothesis, the selected poses for compounds **4**, **5** and **6** were tested for their stability in pocket P9. Furthermore, the interaction of selected poses with ARG77-C was determined for every frame.

Analysis: For the analysis of the MD simulation, the trajectory was aligned based on the protein. The root mean square deviation (RMSD) was calculated to assess the deviation of atom positions compared to the starting pose over time. Furthermore, distances between the interacting protein and ligand atoms for the hydrogen bond were tracked over the whole trajectory.

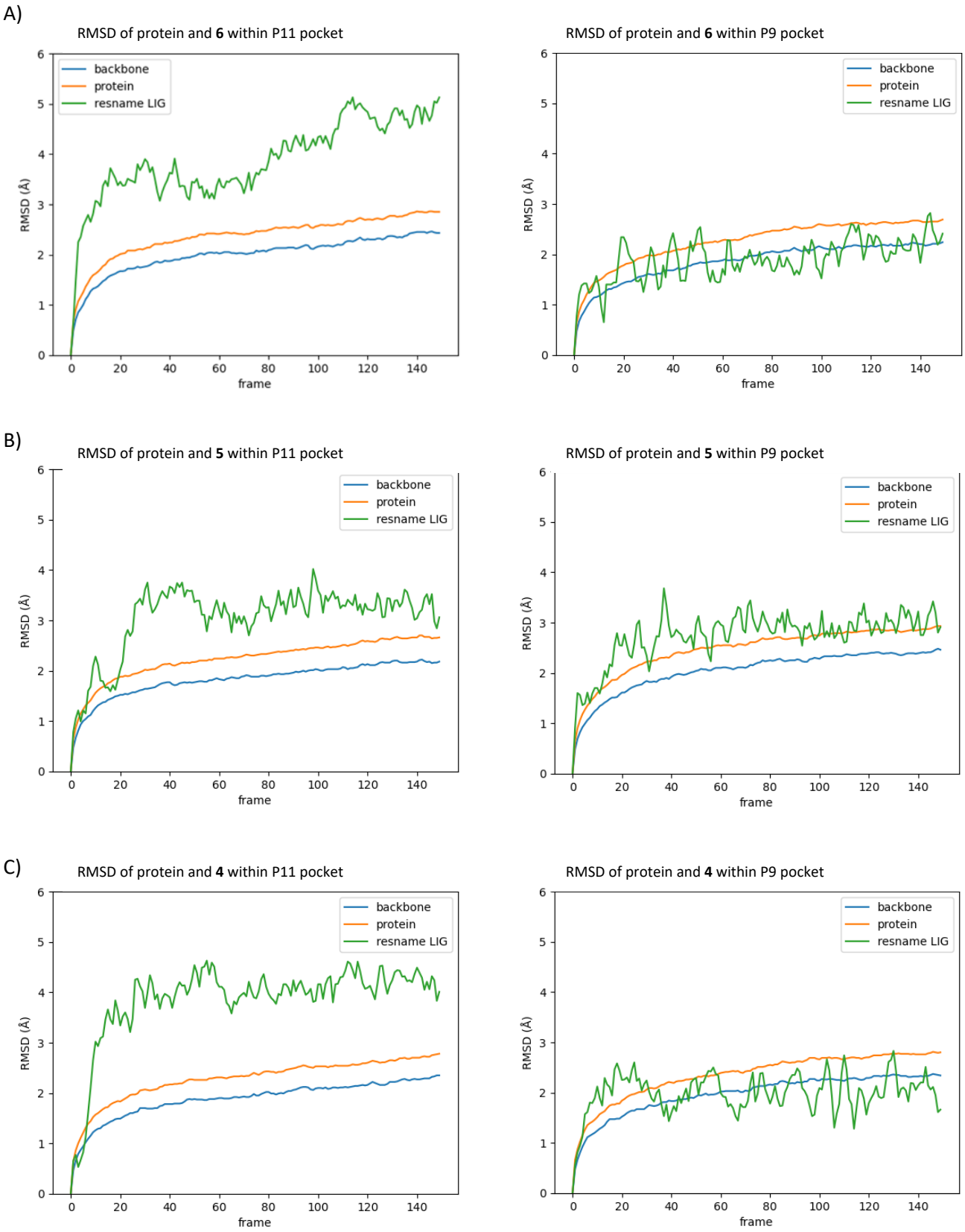

Figure S8. Binding pocket difference: Stability of the high scoring poses in binding pockets P11 and P9 to select the more suitable starting structure for this study. Results are shown for the three compounds: A) **6**, B) **5** and C) **4**. Left: Results for pocket P11, right results for pocket P9.

A) **6** (**A6H19**) **5** (**A5H9**) **4** (**A5H10**)

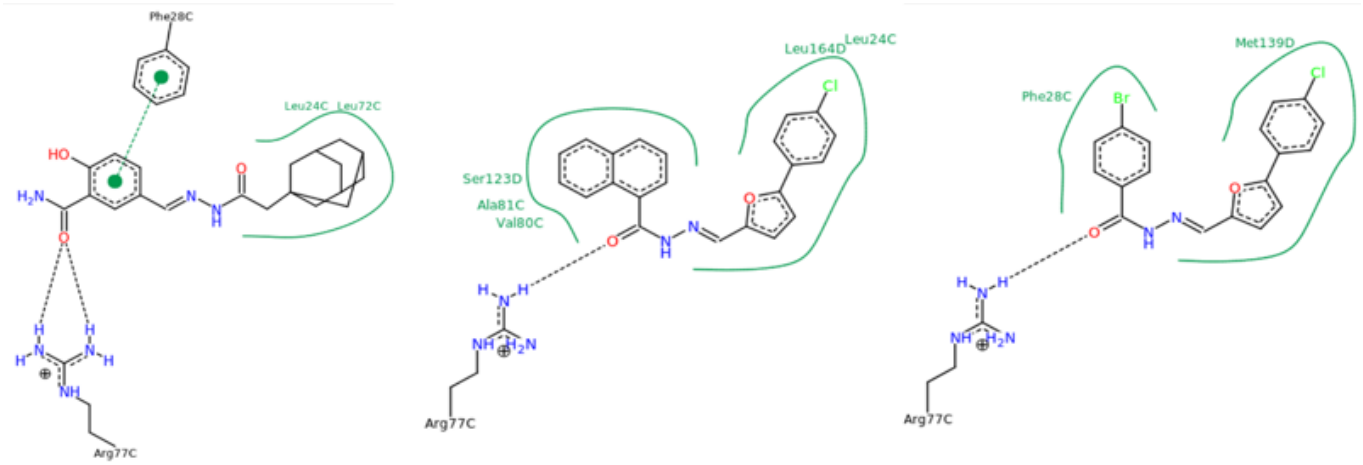

Figure S9. 2D interaction diagrams for the selected poses of the three hit compounds using PoseView.[22]

Compound **1** series: derivatives **6**

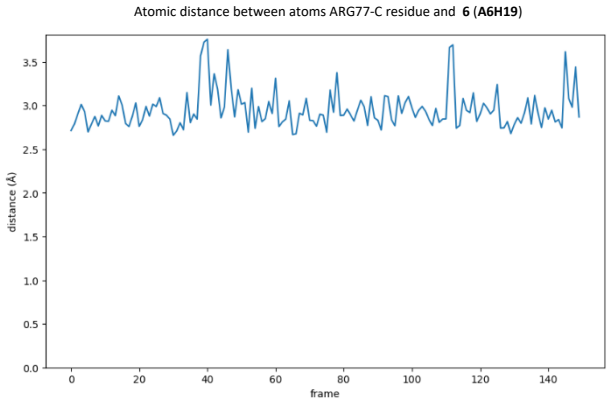

Compound **2** series: derivatives **4** and **5**

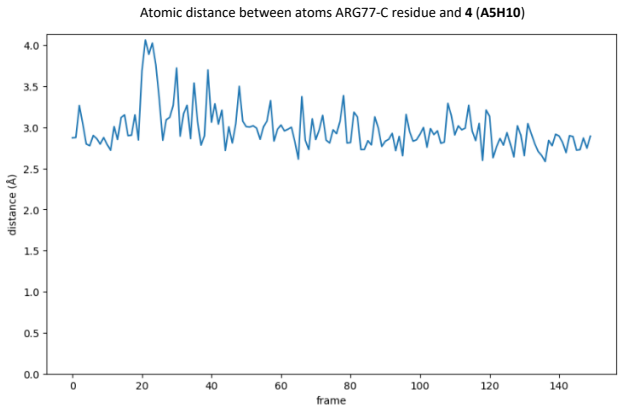

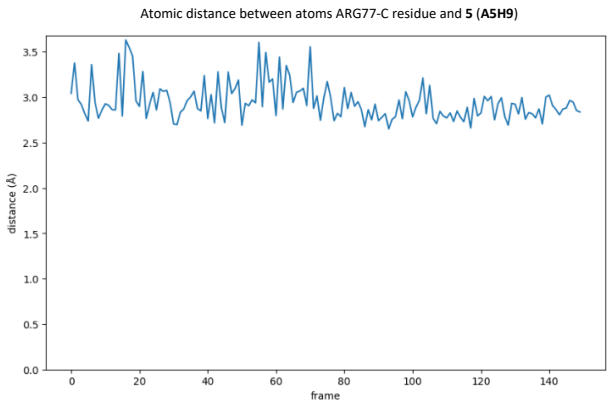

Figure S10. Selected poses and ARG77-C distance: As shown in MD analysis, selected poses remained intact with ARG77-C over the 6 picoseconds.

SUPPLEMENTARY FIGURES

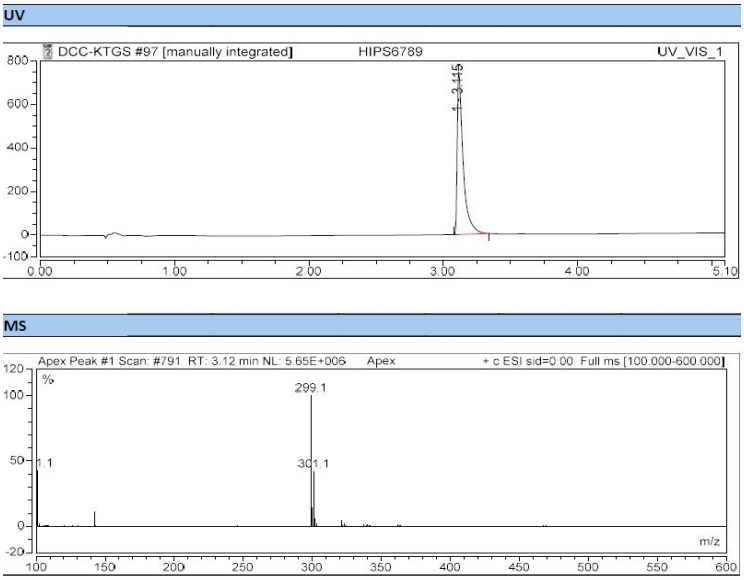

Figure S11. HPLC purity analysis of **A1H5**.

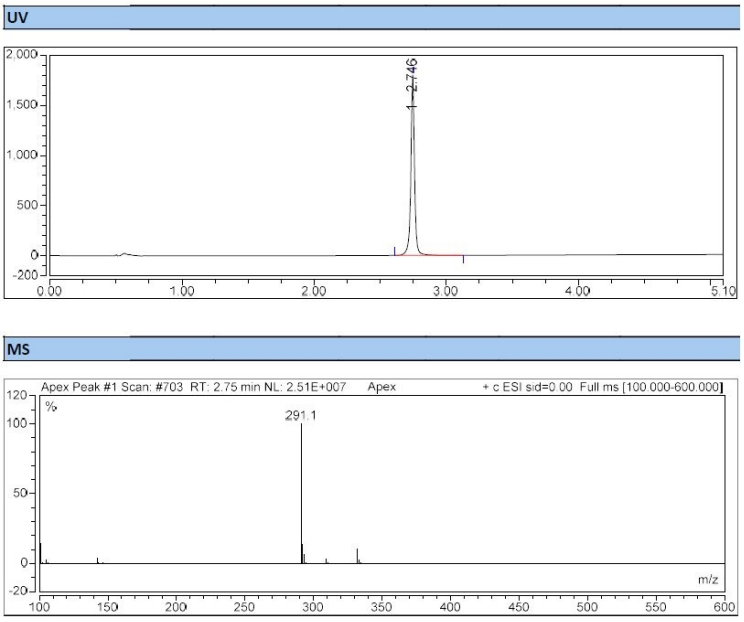

Figure S12. HPLC purity analysis of **A3H8**.

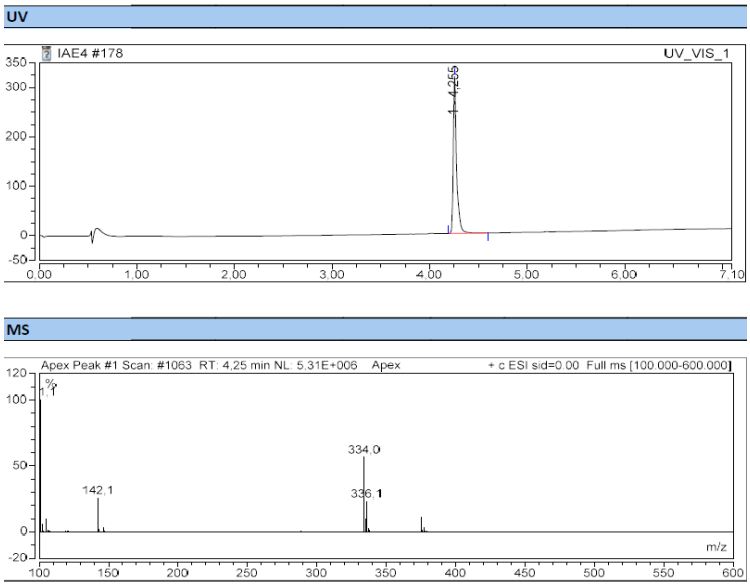

Figure S13. HPLC purity analysis of **A2H5**.

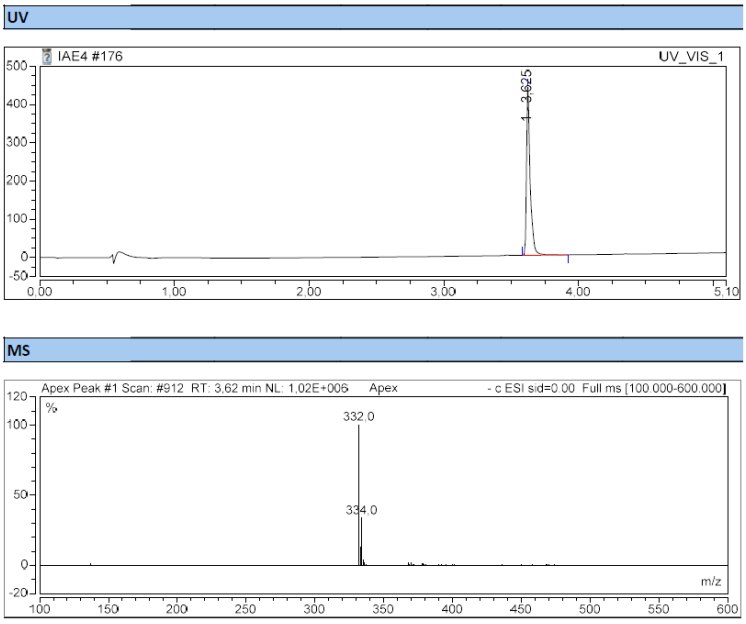

Figure S14. HPLC purity analysis of **A2H6**.

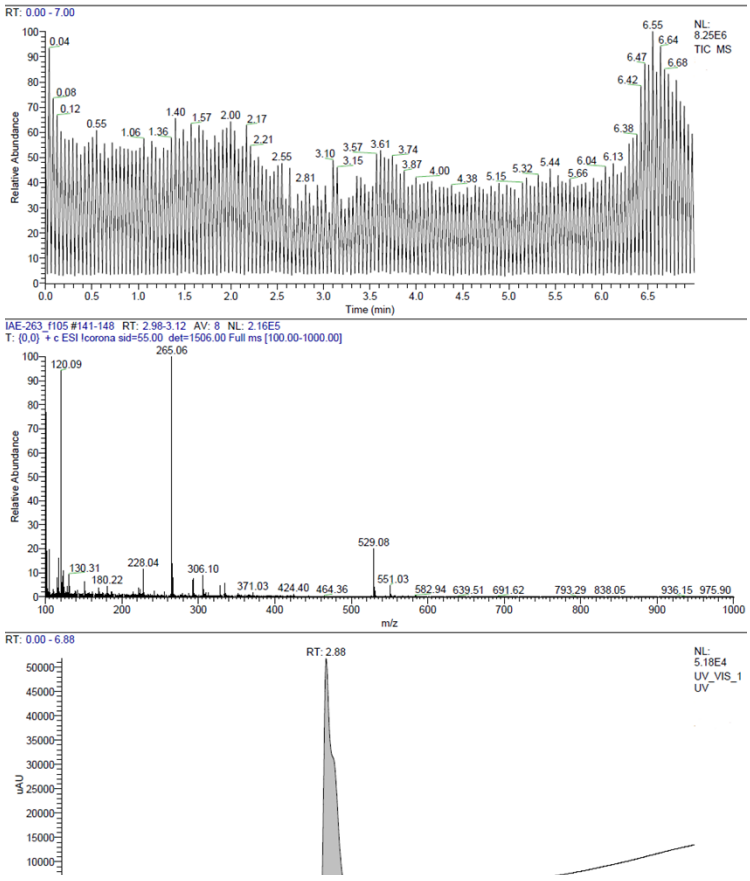

Figure S15. HPLC purity analysis of compound **A1H7** as a mixture of both rotamers.

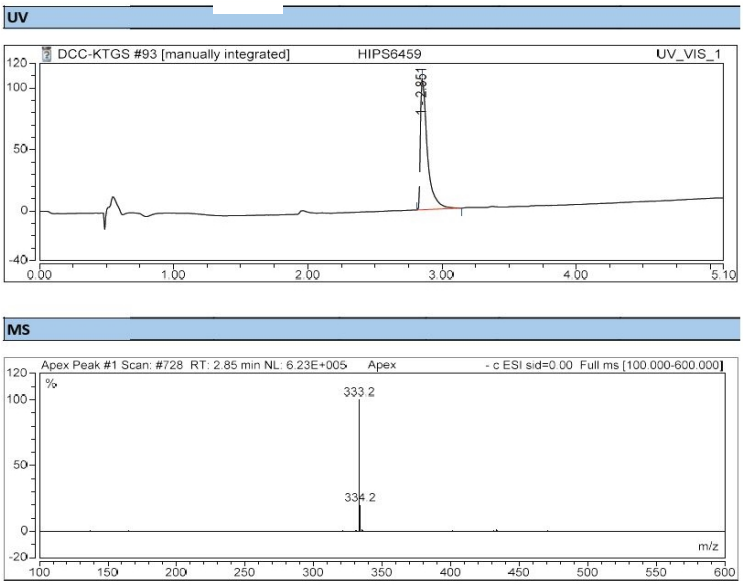

Figure S16. HPLC purity analysis of compound **3** (**A4H9**).

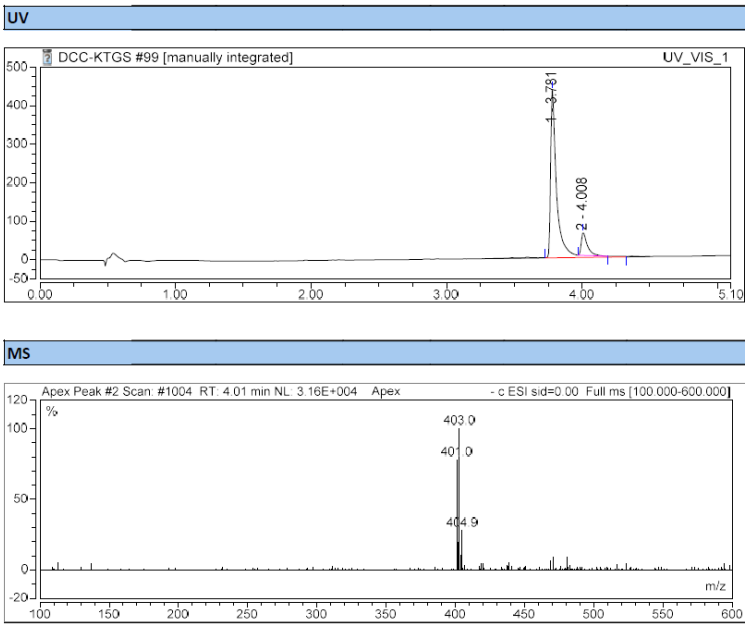

Figure S17. HPLC purity analysis of compound **4** (**A5H10**) as a mixture of both rotamers.

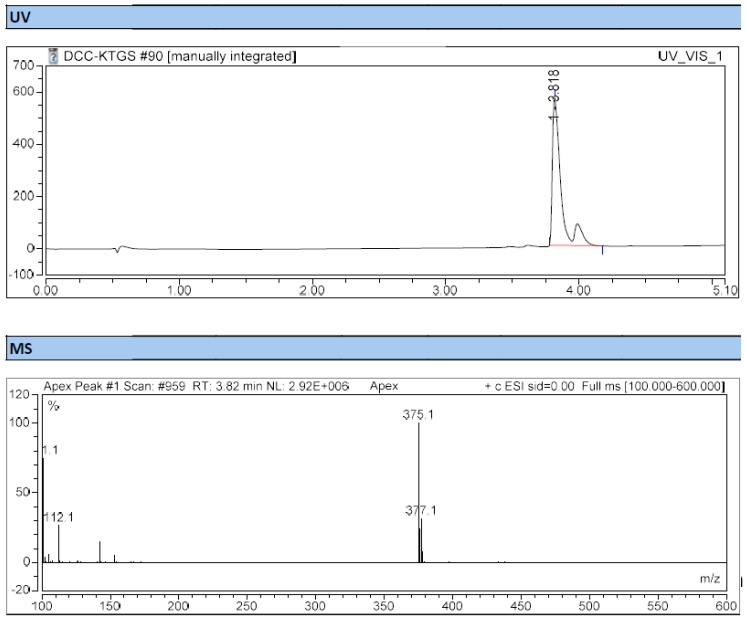

rotamers.

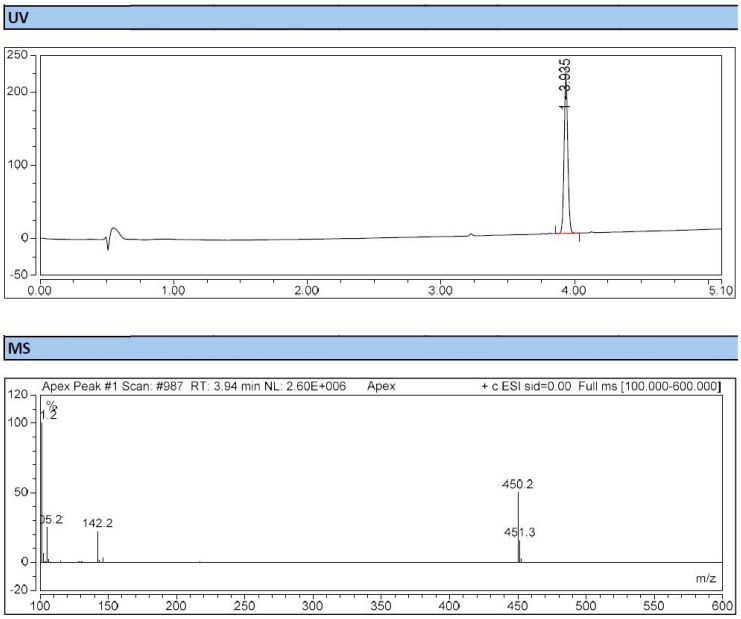

Figure S19. HPLC purity analysis of **A7H15**.

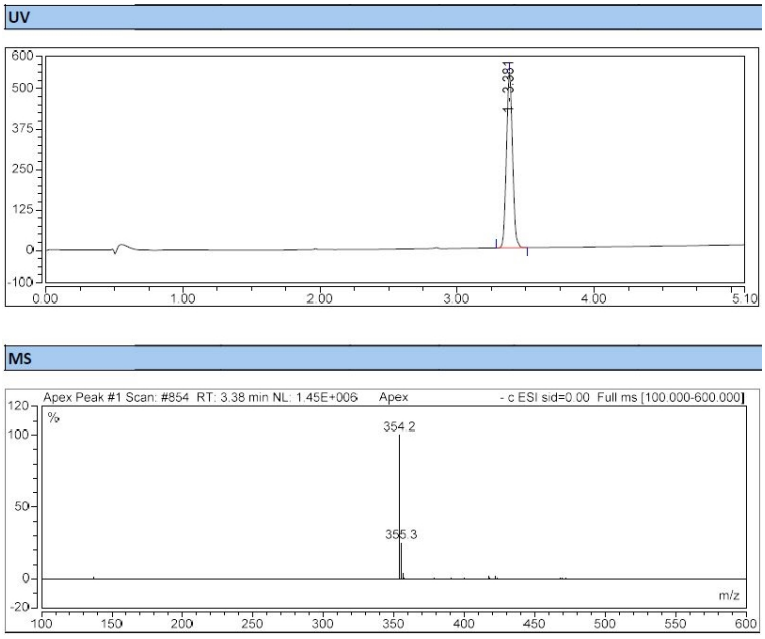

Figure S20. HPLC purity analysis of compound **6** (**A6H19**).

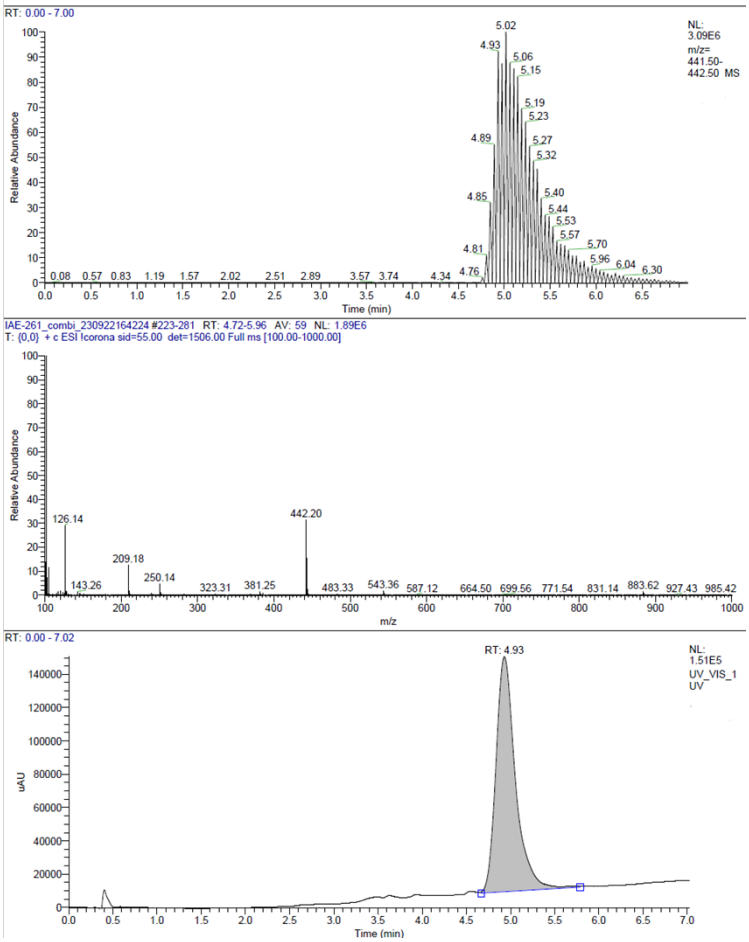

Figure S21. HPLC purity analysis of compound **A7H19**.

Supplementary References

1 R. P. Jumde, M. Guardigni, R. M. Gierse, A. Alhayek, D. Zhu, Z. Hamid, S. Johannsen, W. A. M. Elgaher, P. J. Neusens, C. Nehls, J. Haupenthal, N. Reiling and A. K. H. Hirsch, *Chem. Sci.*, 2021, **12**, 7775−7785.

2 A. Shams, unpublished work.

3 O. Ramström and J. M. Lehn, *Nat. Rev. Drug Discov.*, 2022, **1**, 26–36.

4 M. Durgun, H. Turkmen, M. Ceruso and C. T. Supuran, *Bioorg Med Chem*, 2016, **24**, 982-988.

5 S. N. P. V. V. Syakaev, B. I. Buzykin, S. K. Latypov, W. D. Habicher, A. I. Konovalov, *J. Mol. Struct.*, 2006, **788**, 55-62.

6 T. L. M. S. F. Altschul, A. A. Schäffer, J. Zhang , Z. Zhang, W. Miller and D. J. Lipman, *Nucleic Acids Res*. 1997, **25**, 3389–3402

7 J. C. W. S. F. Altschul, E. M. Gertz, R. Agarwala, A. Morgulis, A. A. Schäffer, Yi. K. Yu, *FEBS J.*, 2005, **272**, 5101–5109.

8 P. Di Tommaso, S. Moretti, I. Xenarios, M. Orobitg, A. Montanyola, J. M. Chang, J. F. Taly and C. Notredame, *Nucleic Acids Res*., 2011, **39**, W13−W17.

9 C. Notredame , D. G. Higgins and J. Heringa, *J. Mol. Biol.*, 2000, **302**, 205−217.

10 Tutorial: How to generate a publication-quality multiple sequence alignment, https://labs.mcdb.ucsb.edu/weimbs/thomas/sites/labs.mcdb.ucsb.edu.weimbs.thomas/files/docs/multiplesequencealignmenttutorial.pdf.

11 L. J. Swier, A. Guskov and D. J. Slotboom, *Nat. Commun.*, 2016, **7**, 11072.

12 S. Bousis, S. Winkler, J. Haupenthal, F. Fulco, E. Diamanti and A. K. H. Hirsch, *Int. J. Mol. Sci.*, 2022, **23**.

13 J. Haupenthal, C. Baehr, S. Zeuzem and A. Piiper, *Int. J. Cancer.*, 2007, **121**, 206-210.

14 E. Diamanti, P. C. T. Souza, I. Setyawati, S. Bousis, L. M. Gómez, L. J. Y. M. Swier, A. Shams, A. Tsarenko, W. K. Stanek, M. Jäger, S. J. Marrink, D. J. Slotboom and A. K. H. Hirsch, *Communications Biology*, 2023, **6**, 1182.

15 SeeSAR version 13.0.3 BioSolveIT GmbH, Sankt Augustin, Germany, 2023.

16 N. Schneider, G. Lange, S. Hindle, R. Klein and M. Rarey, *J. Comput. Aided Mol. Des*., 2013, **27**, 15−29.

17 P. Eastman ,J. Swails, J. D. Chodera, R. T. McGibbon, Y. Zhao, K. A. Beauchamp, L. P. Wang, A. C. Simmonett,M. P. Harrigan, C. D. Stern, R. P. Wiewiora, B. R. Brooks and V. S. Pande, *PLoS Comput. Biol.,* 2017, **13**, e1005659.

18 Landrum, G. 2010. “RDKit.” Q2. https://www.rdkit.org/.

19 J. Wang, R. M. Wolf, J. W. Caldwell, P. A. Kollman and D. A. Case, *J. Comput. Chem.*, 2004, **25**, 1157−1174.

20 W. L. Jorgensen, J. Chandrasekhar, J. D. Madura; R. W. Impey and M. L. Klein, *J. Chem. Phys.*, 1983, **79**, 926–935

21 J. A. Izaguirre C. R. Sweet and V. S. Pande, *Pac Symp Biocomput.*, 2010, 240−251.

22 K. Stierand and M. Rarey, *ACS Med. Chem. Lett.*, 2010, **1**, 540–545.